

# The Future of Neuroimplantable Devices: A Materials Science and Regulatory Perspective

Nikita Obidin, Farita Tasnim, and Canan Dagdeviren\*

The past two decades have seen unprecedented progress in the development of novel materials, form factors, and functionalities in neuroimplantable technologies, including electrocorticography (ECoG) systems, multielectrode arrays (MEAs), Stentrode, and deep brain probes. The key considerations for the development of such devices intended for acute implantation and chronic use, from the perspective of biocompatible hybrid materials incorporation, conformable device design, implantation procedures, and mechanical and biological risk factors, are highlighted. These topics are connected with the role that the U.S. Food and Drug Administration (FDA) plays in its regulation of neuroimplantable technologies based on the above parameters. Existing neuroimplantable devices and efforts to improve their materials and implantation protocols are first discussed in detail. The effects of device implantation with regards to biocompatibility and brain heterogeneity are then explored. Topics examined include brain-specific risk factors, such as bacterial infection, tissue scarring, inflammation, and vasculature damage, as well as efforts to manage these dangers through emerging hybrid, bioelectronic device architectures. The current challenges of gaining clinical approval by the FDA—in particular, with regards to biological, mechanical, and materials risk factors—are summarized. The available regulatory pathways to accelerate next-generation neuroimplantable devices to market are then discussed.

## 1. Introduction

Neuroimplantable devices span a wide range of tools used for recording brain activity,<sup>[1]</sup> stimulating neural networks,<sup>[2,3]</sup> chemosensing,<sup>[3,4]</sup> optical sensing,<sup>[5]</sup> and pinpoint drug delivery with high spatial precision.<sup>[6]</sup> In the last 50 years, neuroimplantable devices have been capable of recording action potentials from the brains of model organisms<sup>[7]</sup> and humans.<sup>[8]</sup> Initially, these experiments only involved single channel recording for short periods of time, typically on the order of hours.<sup>[9]</sup> However, revolutionary progress in materials science has enabled the creation of biocompatible, chronic neuroimplantable devices, partially through conformable mechanics,

flexible substrates, and novel form factors. Advances in neuroimplantable form factors and fabrication methods have at present permitted long-term recording of up to years at a time.<sup>[10–12]</sup> Accompanying improvements in fabrication have resulted in a series of medical devices approved by the US Food and Drug Administration (FDA) for a range of diseases.<sup>[7,13–17]</sup>

The development of systems for neural interfacing have spanned nearly a 100 years and have included recording electrodes,<sup>[18]</sup> neural stimulation,<sup>[19]</sup> and transcranial drug delivery,<sup>[6]</sup> as shown in **Figure 1**. Technology to record signals from the human brain has been in existence since the 1930s, with the advent of the noninvasive electroencephalography (EEG)<sup>[3,20]</sup> and the transcranial electrocorticography (ECoG).<sup>[8,21,22]</sup> This was soon followed by the development of a penetrating medium-depth microwire electrode array.<sup>[18]</sup> The first tests of microwire arrays in cell culture occurred in 1972, using myocytes from embryonic chicks.<sup>[23]</sup> Over the following two decades, the advancement of novel materials and fabrication strategies lowered costs and thereby

reduced the barrier-to-entry into the field of neuroimplantables for a greater number of research labs.<sup>[23]</sup> Micromachined silicon-based shanks forming an array of rigid penetrating electrodes emerged in the early 1990s, notably those developed at the University of Michigan (1971)<sup>[24]</sup> and at the University of Utah (1992).<sup>[18,25]</sup> These new designs helped to revolutionize the field and provide new standards for neural interfacing research due to their high density of recording, durability, and relative biocompatibility, especially as a result of pore-free coatings such as parylene.<sup>[26]</sup> Building on top of these designs, the last few decades have seen a wide assortment of new conformable recording modalities, including polymer-based electrodes,<sup>[27]</sup> conducting nanostructures,<sup>[3]</sup> and wireless sensing tools such as neural dust.<sup>[1,28]</sup>

In parallel, implantable devices for augmenting brain function have permitted electrical and chemical modulation of the brain with increasing fidelity. Though electrical stimulation of the brain has been demonstrated in clinical practice since the 1930s for cases of epilepsy, it was not until 1947 that deeper electrical stimulation of subcortical regions became possible.<sup>[29]</sup> In patients with motor disorders, it was noted that lower frequency stimulation of particular areas could exacerbate symptoms,

N. Obidin, F. Tasnim, Prof. C. Dagdeviren  
MIT Media Lab  
Massachusetts Institute of Technology  
Cambridge, MA 02139, USA  
E-mail: canand@media.mit.edu

 The ORCID identification number(s) for the author(s) of this article can be found under <https://doi.org/10.1002/adma.201901482>.

DOI: 10.1002/adma.201901482

while higher frequencies could reduce symptoms, though most experimentation with stereotactic surgery was for the purpose of ablation.<sup>[19,30]</sup> In patients with Parkinson's disease (PD), the subthalamic nucleus (STN), now the main target for deep brain stimulation (DBS), was identified as one such area.<sup>[19]</sup> With the introduction of the dopamine precursor levodopa in 1968, deep probe implantation for DBS became less common.<sup>[31]</sup>

Additionally, a public campaign against the use of stereotactic surgery for brain stimulation waned and nearly faded into obsolescence.<sup>[31]</sup> The rebirth of brain augmentation therapies occurred in parallel with the introduction of the first implantable pacemakers by Medtronic, followed by similar neurostimulators for a variety of brain diseases.<sup>[29]</sup> This resulted in the eventual approval of clinical DBS therapy for PD in 2002<sup>[29,32]</sup> and for epilepsy in 2018.<sup>[33]</sup> In the last few years, new tools have appeared which have furthered our ability to interact with the human brain, including through optogenetics<sup>[5,34]</sup> and drug infusion.<sup>[6,35]</sup> These tools have been further enhanced through incorporation of flexible substrates which have reduced the damage to neural tissue.<sup>[36]</sup> These new developments are opening new frontiers for augmenting brain function, elucidating pathways to the treatment of disease and broadening our understanding of neural circuitry.

Despite the emergence of novel tools for neural interfacing, FDA clearance remains a sparsely covered topic in most academic studies of neuroimplantable devices. The FDA considers several main factors in their decision to clear a neuroimplantable device for clinical trials and, thereafter, commercial use. Four integral features especially help a device through the FDA approval process: i) materials choices, ii) form factor, iii) functionality, and iv) implantation procedure. If these features of the device closely match those of previously approved designs, as was the case with the Blackrock Microsystems NeuroPort Microelectrode Array (MEA) System,<sup>[13]</sup> the Accuport Electrode,<sup>[14]</sup> the RTI Surgical, Inc., Nerve Monitoring Cable System,<sup>[15]</sup> and the Longeviti PMMA Static Cranial Implant,<sup>[16]</sup> then the process is markedly smoother. Neural interfaces employing well-known, empirically established material choices, form factors, functionalities, and implantation procedures are better equipped to transition to the clinical phase.<sup>[37]</sup>

## 2. Materials Engineering as a Determinant of Risk Factors and FDA Clearance

Material choices are notably important for FDA approval as they directly affect biocompatibility, toxicity, and long-term histological effects in the brain.<sup>[38,39]</sup> Furthermore, since neural tissue has a soft consistency with an elastic modulus in the range of 0.4–15 kPa,<sup>[40–45]</sup> interfacing to the brain with nonbiological materials like platinum ( $\approx 250$  MPa) and silicon ( $\approx 200$  GPa) creates a huge mismatch in mechanical properties, leading to adverse foreign body responses, such as tissue scarring and motion-related damage to chronic implants.<sup>[46,47]</sup> The FDA has specifically defined guidelines which are relevant to the biocompatibility of materials used in medical devices.<sup>[38]</sup> Certain materials have an extensive list of approved predicates, which may be considered evidence of safety in de novo



**Nikita Obidin** earned his B.S. in chemical engineering from the University of Massachusetts Amherst and is now a graduate student in the Conformable Decoders Group at the MIT Media Lab. His research focus is on the development and fabrication of novel multimodal neuro-implantable devices for early diagnosis of brain diseases.

His previous work focused on tools for high resolution spatial mapping of the transcriptome.



**Farita Tasnim** earned her B.S. in electrical engineering from the Massachusetts Institute of Technology and is now a Ph.D. student in the Conformable Decoders group at the MIT Media Lab. Her research focuses on the intersection between energy harvesting, sensing, and biological integration, so as to create conformable hybrid,

self-powered sensors for continuous monitoring of longitudinal health patterns.



**Canan Dagdeviren** is an assistant professor of Media Arts and Sciences and LG Career Development Professor of Media Arts and Sciences at Massachusetts Institute of Technology, where she leads a research group, called Conformable Decoders. Prof. Dagdeviren earned her Ph.D. in materials science and engineering from the

University of Illinois at Urbana-Champaign. Her collective research aims to design and fabricate conformable, hybrid electromechanical systems to convert the patterns of nature and the human body into beneficial signals and energy.

devices. Examples of approved predicate materials include silicon, parylene-C, polydimethylsiloxane (PDMS), platinum, and iridium.<sup>[48]</sup>

In addition to these materials, many novel coatings have been tested to reduce the foreign body response, especially glial scarring, occurring at neural interfacing sites in vivo. Since glial scarring develops at least in part due to the micromotions of relatively stiff implanted components with respect to soft brain

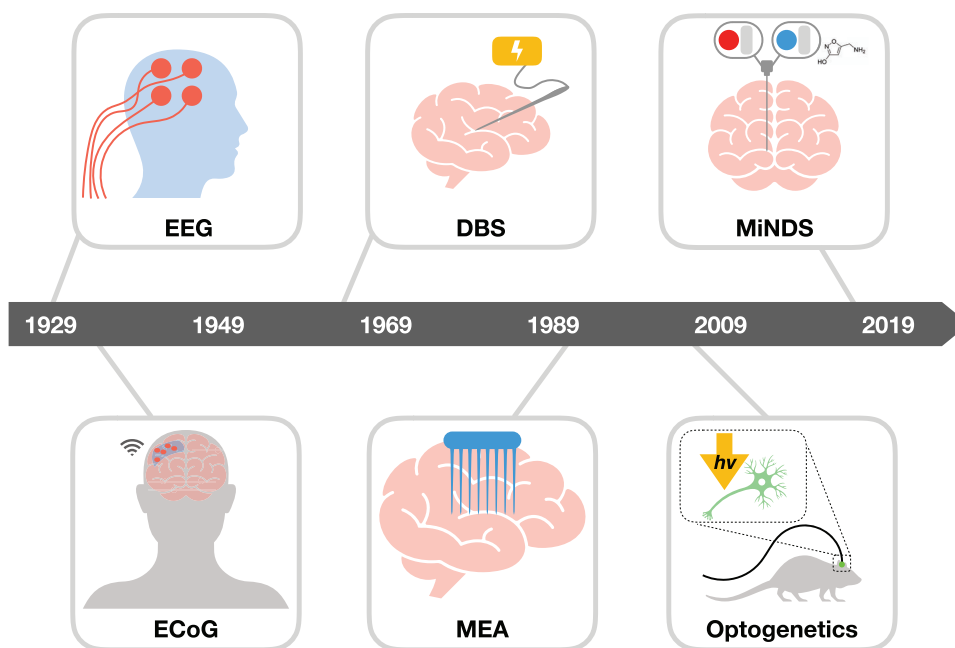


**Figure 1.** A timeline of developments in brain-interfacing technologies, highlighting their first recorded uses in research. 1) Noninvasive electroencephalography (EEG) which permits recording with nonpenetrating leads. 2) Invasive electrocorticography (ECoG) which allows for transcranial recording with nonpenetrating leads placed above or below the dura. 3) Implanted penetrating probes for deep brain stimulation (DBS). 4) Multielectrode arrays (MEA) consisting of high numbers of penetrating electrodes permitting recording from a larger region of the cortex. 5) Optogenetics for the activation of neural networks using light from penetrating electrodes. 6) Miniaturized neural drug delivery systems (MiNDS) for precise delivery of therapeutics into deep brain regions.

tissue, researchers have coated rigid, silicon-based devices ( $\approx 200$  GPa modulus) with polyethylene glycol dimethylacrylate (PEG-DMA) ( $\approx 15$  kPa) in order to dampen local strain fields.<sup>[49]</sup> Their results indicate that hydrogel coatings on rigid probes can improve biocompatibility and reduce the effects of micromotions. In another case, Matrigel, dexamethasone (DEX), nerve growth factor (NGF), and brain-derived neurotrophic factor (BDNF) were used to coat a parylene and platinum-based probe, resulting in a higher signal-to-noise ratio (SNR), which improved device functionality.<sup>[50]</sup> Researchers have also demonstrated the feasibility of creating insertion shuttles made of bioresorbable polymers, such as polyvinyl alcohol (PVA) and poly(lactic-co-glycolic acid) (PLGA), to reduce glial scarring during implantation of rigid probes.<sup>[51]</sup> For polymer-based probes, such as those coated parylene-C as the substrate material, that are too flexible to be implanted directly into the brain, silk coatings have been used during implantation to act as a temporary stiffening agent which dissolves in the brain afterward.<sup>[52]</sup> Another study showed that coatings made of extracellular matrix (ECM) hydrogels, such as collagen and fibronectin, improve chronic biocompatibility of subdural ECoG arrays.<sup>[53]</sup>

While coatings can improve the biocompatibility and signal-to-noise ratio of a neuroimplantable device, neural foreign body response hinges more crucially on the form factor and material choices for a neuroimplantable device. **Figure 2** summarizes the existing state of neuroimplantable devices, where each device is depicted with its target region in the brain, along with its form factor and materials choices. It shows representative examples of FDA-approved devices as well as several devices that are still in the research phase. FDA-approved, commercial neuroimplantable

devices—such as the Utah array<sup>[54]</sup> and DBS probes<sup>[32,33]</sup>—have been proven as viable for chronic implantation in the human brain. Neural interfaces reported in academic literature that are similar to FDA-approved devices, yet offer additional functionalities and novel form factors—such as conformability, drug delivery, and bioresorbability—have yet to commence clinical trials. The following section will explore the materials used in such devices of various forms and functionalities, organized by implantation procedure, and specifically penetration depth.

## 2.1. Electrocorticography Arrays

Neuroimplantable devices with the least intracranial penetration are known as ECoG arrays. **Figure 3** exhibits the various FDA-approved ECoG arrays and noncommercial, research-phase ECoG arrays. The following section outlines the evolution of subdural ECoG arrays, as well as current research progress in advancing ECoG to include mechanically adaptive and bioresorbable form factors and better functionality in terms of lower electrode impedance and higher charge injection capacity, signal-to-noise ratio, and signal coherence.

### 2.1.1. FDA-Approved ECoG Arrays

Electrocorticography has been explored by researchers for several decades, led along mostly by an effort to demystify the onset, progression, and treatment of epilepsy. The very first electrocorticogram was demonstrated by Foerster

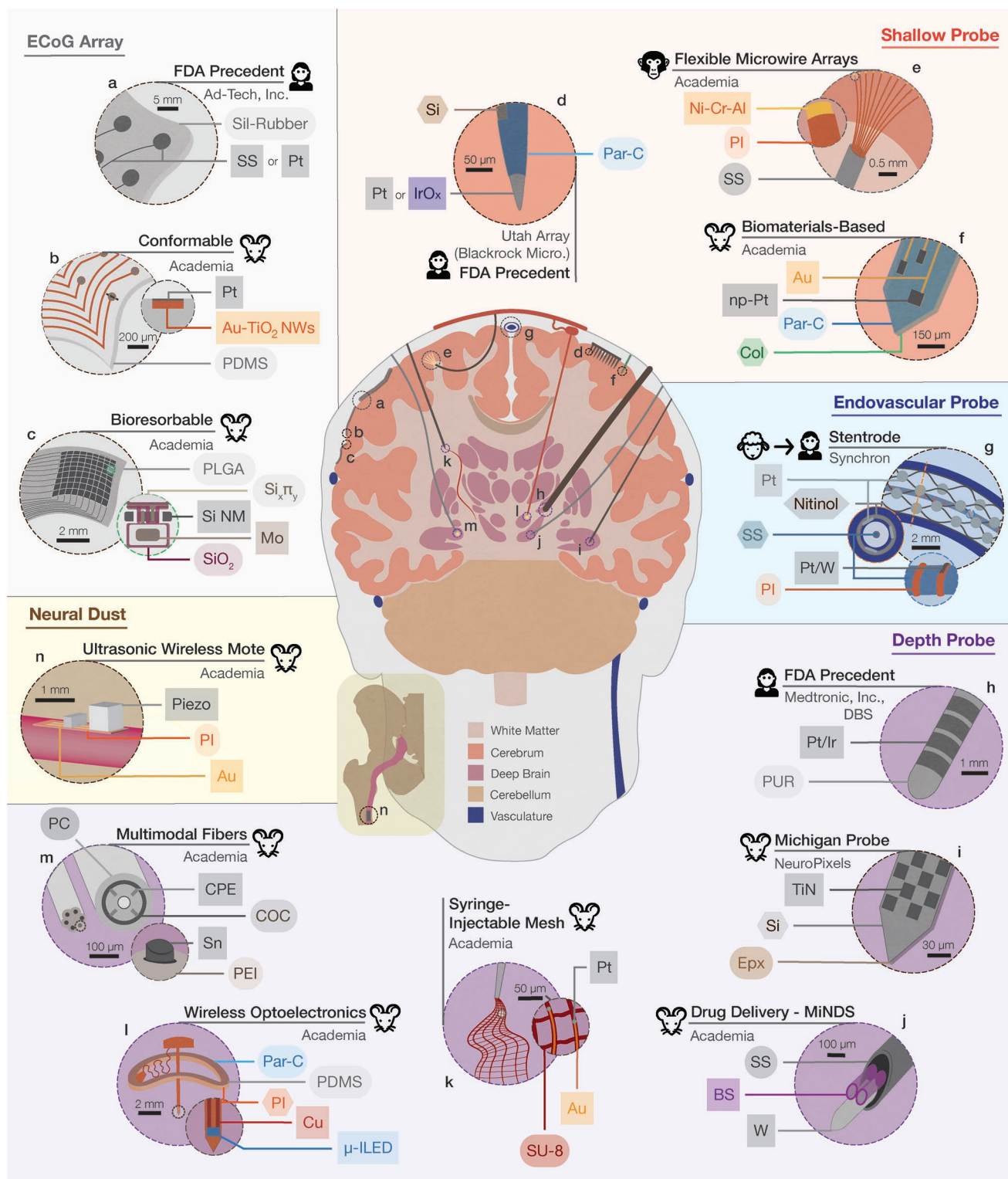


**Figure 2.** A summary of neuroimplantable devices, including FDA-approved devices, labeled “FDA Precedent,” recent progress in academic literature, labeled “Academia,” and commercially available probes for nonhuman research purposes, labeled with the company name, such as “Synchron” or “NeuroPixels.” Probe Types: Devices are organized by depth of penetration into the brain: subdural ECoG arrays, shallow probes, endovascular probes, depth probes, and neural dust, which is for the peripheral nervous system. For each type of probe, one FDA precedent and a few research-phase advancements are shown. Each of the probes is shown penetrating into its target region on the cross section of the human skull, brain, and cerebral vasculature. Additionally, the sciatic nerve in the hip-leg area is depicted to show the placement of neural dust. Probe constituent materials are noted with callouts. Material Types: The rectangular shape indicates electrode or photonic material; the pill shape indicates encapsulation, insulation,

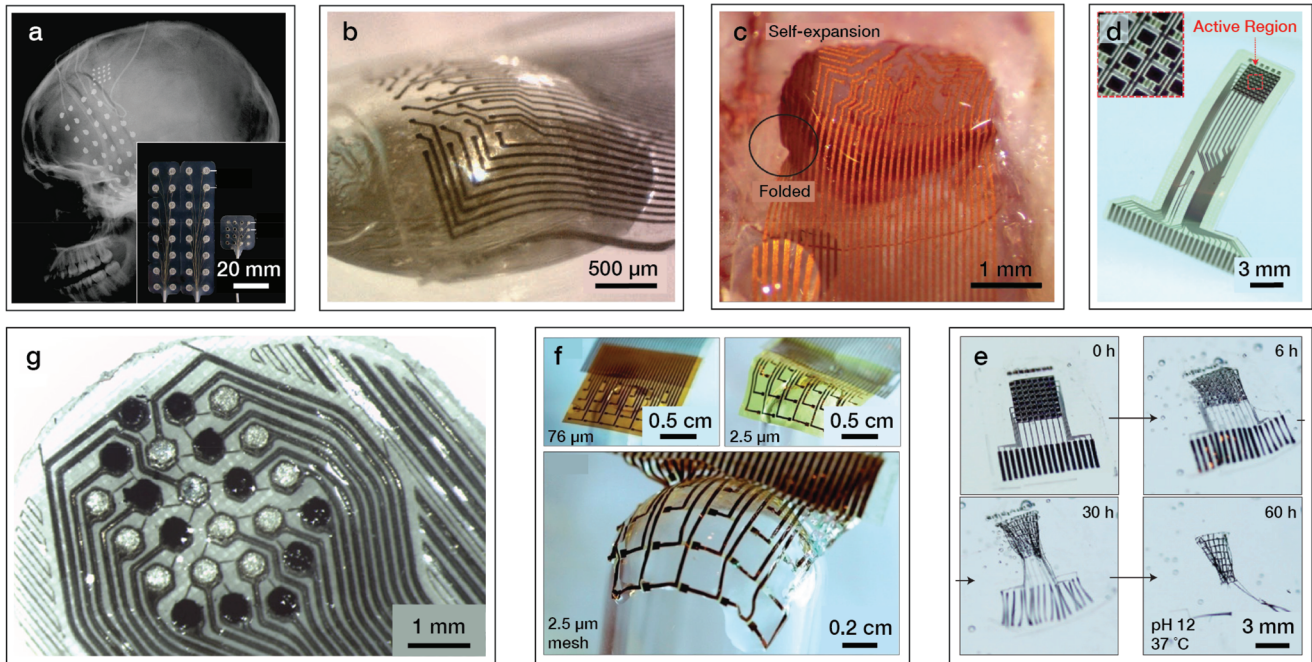


**Figure 3.** A summary of subdural ECoG arrays made of various materials and representing different functionalities. a) Standard commercial ECoG array by Ad-Tech, Inc. compared to a micro-ECoG array by the same company. High-density micro-ECoG arrays are currently being evaluated for viability in clinical trials.<sup>[64]</sup> Adapted with permission.<sup>[65]</sup> Copyright 2009, IEEE. b, c) Conformable micro-ECoG array shown laminated to a curvilinear surface in (b) and unfolding and self-expanding onto the cortical surface of a rat brain in (c). Adapted under the terms of the CC-BY-NC license.<sup>[56]</sup> Copyright 2018, the Authors. Published by Wiley. d, e) Bioresorbable monocrystalline silicon nanomembrane micro-ECoG array and multiplexers (d) shown dissolving in an accelerated fashion in pH 12 buffer solution (e). Adapted with permission.<sup>[57]</sup> Copyright 2016, Springer Nature. f) Conformable ECoG array made with dissolvable silk fibroin film. Top left: Undissolved silk fibroin layer under solid substrate. Top right: Dissolved silk fibroin layer under solid substrate. Bottom: Dissolved silk fibroin layer under mesh substrate. Adapted with permission.<sup>[66]</sup> Copyright 2010, Springer Nature. g) Platinum-coated PEDOT:pTS electrodes (dark) and bare platinum electrodes (light) in a multimaterial array for comparison of material performance and stability for cortical stimulation. Adapted with permission.<sup>[67]</sup> Copyright 2013, IOP Publishing Ltd.

and Altenburger in 1935.<sup>[21]</sup> Thereafter, one of the first subdural ECoG array devices was made by Jasper and Penfield in 1949.<sup>[68]</sup> They used eight electrodes, each consisting of a flexible silver wire with a fused ball tip. The electrode wires were encapsulated in a plastic varnish. After a craniotomy, the electrodes were mounted directly onto a normal human cerebral cortex in order to analyze signals from the precentral gyrus, *in vivo*.

Since that landmark study, a few commercial ECoG devices have been approved by the FDA for subchronic implantation

for presurgical diagnosis of epilepsy.<sup>[55,69–71]</sup> One such device (Ad-Tech Inc.), depicted in Figure 2a, comprises of a grid of 32 disc-shaped 3 or 4 mm diameter platinum (or stainless steel) electrodes spaced 10 mm apart and encapsulated in silicone rubber.<sup>[55,65]</sup> Though ECoG is implanted through a procedure requiring an invasive craniotomy, it remains preferred over EEG/MEG and MRI for epileptic patients, due to its empirical reliability in localized identification of epileptogenic brain tissue and mapping of primary brain functions for guidance during surgery.<sup>[72]</sup>

dielectric, or coating material; and the hexagonal shape indicates substrate or foundational material. *In vivo* trials: The animal icons next to each device name indicate the most recent *in vivo* trials (rodent, sheep, and nonhuman primate preclinical, and human clinical) in which the device has been tested. The Stentrode's sheep to human animal label indicates that the device is currently transitioning from preclinical trials with sheep to clinical trials with humans. ECoG Array: The subdural ECoG array is represented by a) Ad-Tech's commercial ECoG array,<sup>[55]</sup> b) a high-density conformable ECoG array,<sup>[56]</sup> and c) a high-density, bioresorbable, multiplexed ECoG array.<sup>[57]</sup> Shallow Probe: The shallow probe is represented by d) BlackRock Microsystems' Utah array,<sup>[13]</sup> e) a flexible microwire array,<sup>[10]</sup> and f) a biomaterial-based intracortical probe.<sup>[58]</sup> Endovascular Probe: The endovascular probe is represented by its only existing device, which is currently undergoing preparation to start clinical trials, g) the Stentrode.<sup>[59]</sup> Depth Probe: The depth probe is represented by h) Medtronic, Inc.'s standard, FDA-approved deep brain stimulation probe,<sup>[32,33]</sup> i) an ultrahigh density Michigan-style NeuroPixels probe,<sup>[60]</sup> j) a miniaturized neural drug delivery system (MiNDS),<sup>[6]</sup> k) a syringe-injectable mesh electrode array,<sup>[61]</sup> l) a seamless, wireless optoelectronics platform,<sup>[62]</sup> and m) multimodal thermally drawn fibers.<sup>[63]</sup> Neural Dust: Neural dust is represented by its only manifestation, in the peripheral nervous system, with n) an ultrasonic wireless mote.<sup>[28]</sup> Abbreviations: Pt: platinum, Ir: iridium, Au: gold, W: tungsten, Si: silicon, Mo: molybdenum, Cu: copper, Sn: tin, IrOx: iridium oxide, TiN: titanium nitride, SiO<sub>2</sub>: silicon dioxide, Si<sub>3</sub>N<sub>4</sub>: silicon nitride, SiO<sub>2</sub>/Si<sub>3</sub>N<sub>4</sub>/SiO<sub>2</sub>: silicon dioxide/silicon nitride/silicon dioxide, Si NM: monocrystalline silicon nanomembrane, SS: stainless steel, Ni–Cr–Al: nickel–chrome–aluminum alloy, BS: borosilicate, np–Pt: nanoporous platinum, Au–TiO<sub>2</sub> NWs: gold-coated titanium dioxide nanowires,  $\mu$ -ILED: micro inorganic light-emitting diode, Nitinol: nitinol, Par-C: parylene-C, PI: polyimide, PUR: polyurethane, Ep: epoxy, Col: collagen, Sil-Rubber: silicone rubber, PDMS: polydimethylsiloxane, SU-8: SU-8 epoxy, PLGA: poly(lactic-co-glycolic) acid, CPE: chlorinated polyethylene, COC: cyclic olefin copolymer, PEI: polyethylenimine. Figure not to scale.

The next wave of ECoG devices making their way to clinical trials largely encompasses advancements toward smaller electrode sizes, higher electrode density (smaller interelectrode distances), and lower electrode impedance. For example, a “micro-ECoG” grid (Ad-Tech, Inc.) consisting of 16 electrodes with 1.5 mm diameter, and spaced 4 mm apart, is shown in Figure 3a alongside a standard-size Ad-Tech ECoG array after implantation into the human skull. Such high-density, micro-ECoG arrays are being evaluated in clinical trials.<sup>[64]</sup> The standard-size and micro-ECoG array use the same materials. Preliminary studies have shown, however, that the micro-ECoG array provides sufficient spatio-temporal resolution, as well as signal integrity and intersignal coherence comparable to standard ECoG, to achieve high accuracy for identification of individual finger movements.<sup>[65]</sup> This study suggests that smaller form factors of ECoG could serve as a potentially viable replacement for traditionally larger ECoG arrays.

To manufacture such commercial ECoG devices, each platinum or stainless steel electrode contact is spot-welded onto microwires of the same material, which are insulated in silicone rubber formed by injection molding.<sup>[72]</sup> This fabrication technique works for a minimum interelectrode distance of 3 mm. Due to their use of relatively large, thick platinum electrodes packed in high density on PDMS, commercial ECoG devices lack the conformability required for intimate contact to the highly irregular, curvilinear surface of the cortex. To create ECoG arrays with higher resolution of electrophysiological recording and greater conformability, different fabrication techniques are required. For example, directly embedding microwires in silicone rubber allows for higher-density ECoG measurements but at the sacrifice of conformability. This is because the microwires, rather than the silicone rubber, begin to dominate the mechanical stiffness (Young’s modulus) of the device. To create high-density ECoG electrodes without sacrificing conformability, microfabrication techniques such as physical vapor deposition of metal films with nanometer-scale thickness and photolithography, reactive ion etching, and transfer printing of micrometer-scale features, are quite useful.<sup>[46,48,72,73]</sup> Specifically, transfer printing allows for the transfer of sub-micrometer thickness, high-modulus metal films onto flexible substrates such as polyimide, parylene-C, and PDMS, making it an invaluable method for creating miniaturized, conformable neuroimplantable devices.<sup>[74–77]</sup>

### 2.1.2. Nonclinically Approved ECoG Arrays

Using microfabrication, noncommercial ECoG devices have now progressed to flexible, stretchable form factors and higher electrode density with grids thinner than 100  $\mu\text{m}$  and with interelectrode distances of 200  $\mu\text{m}$  or less, while retaining the ability to conform seamlessly to the surface of the cortex. Researchers have demonstrated a 32-electrode array made of Au–TiO<sub>2</sub> nanowire conductors that are embedded in PDMS, except at the contact sites (50  $\times$  50  $\mu\text{m}$  wide, 7  $\mu\text{m}$  deep, 200  $\mu\text{m}$  interelectrode distance), which are electroplated with a thin layer of platinum.<sup>[56]</sup> The final device is depicted in Figure 2b and shown in Figure 3b. At 80  $\mu\text{m}$  thickness, it can i) bend and

fold onto itself, as shown in Figure 3c, for insertion through a craniotomy window 30% narrower than its size, ii) establish conformal contact onto the pial cortical surface, and iii) remain chronically implanted and functional for at least three months. While the choice of PDMS as encapsulation material follows the examples of commercial ECoG devices,<sup>[55]</sup> the specific choice of Au-coated TiO<sub>2</sub> nanowires for electrode material allows for improved long-term electromechanical stability (after 1000 strain cycles of 100% strain), ease of use, biological benignity, high electrode density, low impedance (10 k $\Omega$  at 1 kHz in phosphate-buffered saline (PBS)), and high areal capacitance (2.7 mC cm<sup>-2</sup>).<sup>[56]</sup>

Microfabrication techniques have also paved the way for the creation of bioresorbable, conformable ECoG devices.<sup>[47,57,78]</sup> Since these devices can be absorbed by body, namely in the cerebrospinal fluid (CSF), without any harmful biological effects, they reduce the risks and complications associated with the additional surgery required to remove standard ECoG devices from the brain. For instance, standard devices may adhere to cortical tissue due to an inflammatory response evoking glial agglomeration.<sup>[3,46]</sup> This phenomenon greatly increases the danger associated with removing devices from the cortical surfaces, but it can be abetted by a bioresorbable form factor.

Researchers have demonstrated one such active bioresorbable device, which is depicted in Figure 2c and shown in Figure 3d, whose 64 electrodes are made with monocrystalline silicon nanomembranes (Si NMs).<sup>[57]</sup> Upon immersion in biofluids, Si NMs undergo hydrolysis, releasing biocompatible byproducts such as silicic acid. The 300 nm thick phosphorous-doped Si NM electrodes (dissolution rate: 11 nm d<sup>-1</sup> in 37 °C, pH 7.4 artificial cerebrospinal fluid (aCSF)) are shielded from biofluids and tissue with an interlayer of 100 nm thick SiO<sub>2</sub> (8.2 nm d<sup>-1</sup>), and encapsulated in 30  $\mu\text{m}$  thick PLGA (8.2 nm d<sup>-1</sup>). The Si NMs, in addition to Mo, SiO<sub>2</sub>, and SiO<sub>2</sub>/Si<sub>3</sub>N<sub>4</sub>/SiO<sub>2</sub>, serve as the material for backplane electronics, such as the 128 metal-oxide-semiconductor field-effect transistors (MOSFETs), required for active multiplexing of the electrodes. In vitro accelerated testing showed that the bioresorbable devices in pH 12 PBS dissolved almost entirely after 60 h, as shown in Figure 3e. The devices were also implanted chronically and preserved functionality for 33 d in mice, in vivo, after which they had hydrolyzed seamlessly into the cerebrospinal fluid. Importantly, biocompatibility tests have demonstrated that the bioresorbable ECoG device exhibits a smaller scale of microglial activation as compared to a commercially available Ad-Tech device described in Section 2.1.1. Such studies demonstrate that bioresorbable microscale ECoG devices have the potential to assume the functionality of traditional ECoG systems in a thinner, more conformable, and biologically inert form factor, due to the precision allowed by its fabrication technique, namely microfabrication of biocompatible thin films.

A similar study explored the use of silk fibroin to create dissolvable substrates to create ultrathin ECoG devices.<sup>[66]</sup> Although this device is not wholly bioresorbable, its substrate, silk fibroin, can dissolve over time upon exposure to water or water-based fluid, including cerebrospinal fluid. This microfabricated device allows for intimate, conformal contact between ultrathin electronics on PI mesh substrates ( $\approx$  2.5  $\mu\text{m}$ ) and curvilinear surfaces inside the body. Microfabrication of thin films

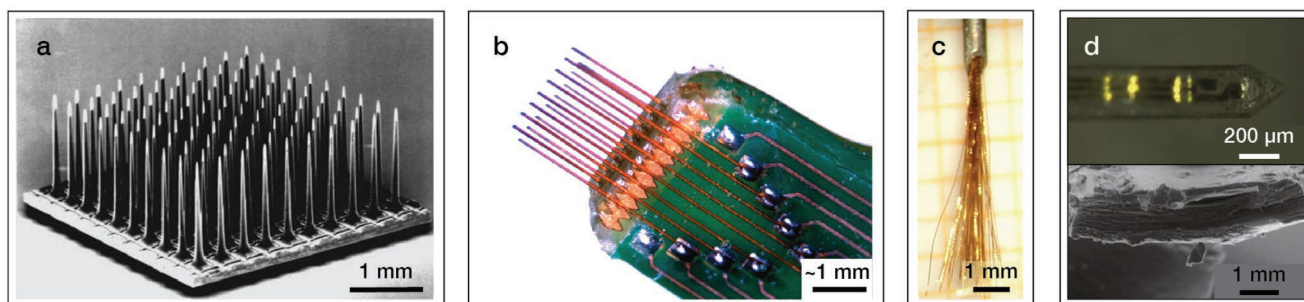


**Figure 4.** A summary of shallow, penetrating probes of various form factors. a) Commercial Utah microelectrode array. Adapted with permission.<sup>[54]</sup> Copyright 2006, Springer Nature, Biomedical Engineering Society. b) Microwire electrode array for research purposes, made by Tucker–Davis Technologies. Adapted with permission.<sup>[80]</sup> Copyright 2009, Elsevier. c) Microwire array implanted for seven years in macaque monkeys. Adapted under the terms of the CC-BY license.<sup>[10]</sup> Copyright 2010, the Authors. Published by Frontiers Media SA. d) Shallow probe made with materials found in the extracellular matrix, such as collagen. Adapted under the terms of the CC-BY-NC license.<sup>[58]</sup> Copyright 2015, the Authors. Published by Springer Nature.

permits the creation of such hybrid interfaces, which serve to reduce mechanical mismatch at the biotic/abiotic interface.<sup>[47]</sup>

Rather than lowering stiffness of materials with microfabrication, another strategy for creating neuroimplantable devices that better match the stiffness of brain tissue is to directly use low-modulus conductive materials such as conductive polymers (CPs), microcomposites, and nanocomposites.<sup>[46]</sup> Such devices are usually fabricated by synthesis, rather than with microfabrication. Researchers have experimented with using CPs, most commonly poly(3,4-ethylene-dioxythiophene) (PEDOT), instead of traditional platinum, iridium, and tungsten electrodes for both electrical recording and stimulation purposes.<sup>[67]</sup> Though many studies have demonstrated viable recording electrodes made with PEDOT doped with poly(styrene sulfonate) (PSS), its limited stability sets PEDOT doped with paratoluene sulfonate (pTS) as the preferred alternative for stimulation. Furthermore, for the device shown in Figure 3f, PEDOT:pTS-coated platinum electrodes (dark) on PDMS substrates were shown to have lower impedance up to 5 kHz and greater charge injection capacity in protein loaded medium ( $1.5\text{--}2.6\text{ mC cm}^{-2}$ ) than bare platinum electrodes (light) on the same substrates ( $0.05\text{--}0.07\text{ mC cm}^{-2}$ ).<sup>[67]</sup> In vivo electrode characterization in a feline model showed greater charge transfer properties in PEDOT:pTS compared to bare platinum, likely due to its higher surface roughness. Another study explored the use of silk fibers as a flexible, natural substrate material combined with PEDOT:pTS electrodes to conduct electrophysiological recording and localized stimulation in vivo in an embryonic chick model.<sup>[79]</sup> The researchers created an array of four 280  $\mu\text{m}$  diameter PEDOT:pTS-coated silk threads, where electrodes had an impedance of  $1.8\text{ k}\Omega\text{ cm}^{-1}$  and an interelectrode distance of 2 mm. With this technique, a novel gamma-band oscillation was revealed in ECoG.

Conductive polymers show promise in improving electrode impedance and charge injection capacity. Since CPs have never been utilized in an FDA-approved neuroimplantable device, however, devices incorporating conductive polymers will require more rigorous in vivo validation in rodent and nonhuman primate models to assure material stability, biocompatibility, and chronic implantation viability<sup>[27]</sup> in order to progress toward clinical trials.

## 2.2. Shallow Probes

While subdural ECoG arrays, which lie on the cortical surface, can only measure surface electrical impulses, shallow probes enable intimate intracortical neural interfacing, recording, and modulation. Since shallow probes can be placed in any intracortical region, they provide a higher signal-to-noise ratio for deeper regions of the cortex, complementing the surface cortical measurements enabled by ECoG arrays. Shallow probes are especially useful for interfacing with neurons in the sensorimotor cortex for the study and treatment of neuromuscular disorders. **Figure 4** exhibits the status of commercially available, FDA-approved shallow probes as well as shallow probes for research trials. The following section outlines several types of shallow probes. Starting with traditional silicon-based microelectrode arrays and microwire arrays, shallow probes have progressed to flexible and chronically implantable or more biocompatible form factors by using novel implantation procedures and microfabrication techniques applied on biological materials. Such improvements have afforded chronic implantation up to seven years<sup>[10]</sup> and reduced foreign body response.<sup>[58]</sup>

### 2.2.1. FDA-Approved Shallow Probes

Researchers have been exploring shallow intracortical probes since the mid-20th century, especially in an effort to create functional neuroprosthetics which are capable of natural motion upon receipt of signals in the motor cortex signifying the intent to move. Commonly, these neuroimplantable devices are referred to as brain-computer interfaces (BCIs). In the 1970s, a landmark study by Wise et al. reported the first Si-based microelectrode fabricated via a complementary metal-oxide semiconductor (CMOS) compatible process.<sup>[81]</sup> Since this pioneering work, Si-based microelectrodes with microscale precision, high repeatability, low unit costs, and various geometries are available and dominant in the studies of neural signal recording.<sup>[82]</sup> The Utah MEA, as one typical example of such a BCI, consists of a  $10 \times 10$  square grid of 1.0–1.5 mm long shank probes with 400  $\mu\text{m}$  spacing.<sup>[83]</sup> As depicted in Figure 2d and shown in Figure 4a, the tip of each shank of the Utah

Array is metalized with sputtered iridium oxide or platinum to enhance conductivity, while the rest of the shank is insulated with a biocompatible and pore-free polymer, parylene-C. The shank length of the Utah MEA is inherently restricted by the thickness of the starting wafer ( $2000 \pm 25 \mu\text{m}$  thick), as the vertical shanks are formed using a top-down wet etching process. The Utah MEA is limited, therefore, by its penetration depth to record brain activity, and is thus primarily used for recording neural signals from superficial cortical tissue. The Utah MEA has been demonstrated both in nonhuman primate models and humans.<sup>[82]</sup> A failure-mode analysis showed that chronically implanted Utah MEAs have an average recording lifetime of 12 months in rhesus monkeys, with the longest successful recording time being 5.75 years.<sup>[12]</sup> Although Utah MEAs have been shown to work chronically in the motor cortex in monkeys, the relative stiffness of the Si shanks compared to neural tissue results in negative foreign body response, such as glial agglomeration.<sup>[46]</sup> Indeed, FDA approval for Blackrock Microsystem's Utah MEA allows for implantation in humans only for a period up to 30 d.<sup>[13]</sup> Potentially longer implantation periods could be enabled by the use of thinner, more flexible probe materials, as is the case with microwire electrode arrays.

### 2.2.2. Nonclinically Approved Shallow Probes

*Microwire Electrode Arrays:* While Utah arrays must be microfabricated from a silicon wafer, microwire arrays are constructed by attachment of a collection of insulated metal wires to a base for electrical recording. Extracellular electrical activity recording for clusters of neurons via microwires has an established history, dating back to the 1950s.<sup>[3]</sup> Initially, metal wire electrodes were used widely in many pioneering studies in neuroscience.<sup>[3]</sup> Typically, a microwire electrode array consists of 16, 32, or 64 metal wires used as unique channels. Each metal wire is electrolytically etched to less than  $100 \mu\text{m}$  in diameter and encapsulated with biocompatible insulating materials, such as polyimide,<sup>[10]</sup> parylene-C,<sup>[84]</sup> Teflon,<sup>[85]</sup> and quartz glass,<sup>[86]</sup> except for at the tip area, which is used as the recording or stimulation site. A broad range of metallic materials have been investigated for the fabrication of metal wire electrodes, including platinum, iridium, platinum-iridium, gold, stainless steel, tungsten, and molybdenum.<sup>[1,87]</sup>

In a rat model, Ward et al. compared the performance for several types of microelectrode arrays over a 31 d period, comparing impedance, charge capacity, signal-to-noise ratio, recording stability, and foreign body response for each probe.<sup>[80]</sup> This study showed that the microwire array from Tucker-Davis Technologies, Inc., (TDT) exhibited the lowest 1 kHz impedance with a mean of  $0.87 \pm 0.04 \text{ G}\Omega \text{ cm}^{-2}$ , compared to the Utah array and Michigan microelectrode system. The TDT MEA, shown in Figure 3b, consists of  $50 \mu\text{m}$  diameter polyimide-insulated tungsten microwires. Interestingly, no failure cases caused by broken connections, damaged connectors, or lost headcap occurred for the metal wire electrodes during the study period, indicating the stability and reliability of the TDT microwire array in terms of products design and mechanical properties. Despite the reduced adverse tissue response to the metal wire electrode, only 30% of recording sites remained

functional after 30 d of implantation, which was similar to Michigan electrode system.<sup>[80]</sup>

The main benefit of the microwire array is the simplicity in its manufacturing process. For example, Takahashi et al. demonstrate fabrication starting with etching a glass substrate by sandblasting to fabricate a master mold and copying the patterns on the master mold onto a thick polystyrene plate.<sup>[88]</sup> After tungsten rods are locked and fixed into the grooves of the patterned polystyrene plate to form a single layer of aligned electrodes, a 3D array is formed by stacking multiple layers and bonding them with pressure and thermal treatment. Eventually, the recording sites on the tip area are exposed via electrodischarge and subsequent electropolishing process. Thus, compared to the microfabrication process of Utah MEAs from a thick silicon wafer, fabrication of microwire electrode arrays is much simpler.

With microwires, however, just as with Utah MEAs, only one recording site is located at the exposed tip of each shank. Hence, increasing the number of recording sites for the microwire array inevitably results in a larger footprint of the overall device and more undesirable neural tissue damage. Furthermore, due to the thin, usually bendable, flexible nature of the wires, it is quite difficult to accurately and precisely position the microwires in the desired target location.

Nevertheless, one study has shown that a microwire electrode array chronically implanted into the ventral premotor cortex of a macaque monkey resulted in stable electrical recordings from one-third of the electrodes for seven years.<sup>[10]</sup> The microwire array, depicted in Figure 2e and shown in Figure 3c, consisted of 64 (initially 100 mm long, and later cut to length),  $12.5 \mu\text{m}$  thick Ni-Cr-Al microwires insulated in  $3 \mu\text{m}$  polyimide. The unique implantation procedure of the microwire array, in which the electrodes penetrate the cortex from the inner white matter side, avoiding the pia mater and most blood vessels, along with its extremely thin form factor, may have led to its success in chronic, accurate electrophysiological readings. Such long-term studies in nonhuman primates are crucial for proving chronic biocompatibility of neuroimplantable devices and pushing along neuroimplantable devices from the research phase to clinical trials and then onto a commercial, FDA-approved status.

*Biomaterial-Based Probes:* Specifically to improve biocompatibility of neural interfacing methods, many of the recent efforts in BCI research focus on methods of reducing the foreign body response of neuroimplantable devices.<sup>[3,46]</sup> One avenue of improvement seeks to match probe materials with biofilms native to the brain, such as those found in the ECM, primarily composed of laminin, fibronectin, and collagen. Researchers have shown that a collagen-based intracortical microelectrode ( $310 \mu\text{m}$  width, 2 mm length) can reduce overall foreign body response in an in vivo rat model.<sup>[58]</sup> This microelectrode, depicted in Figure 2f and shown in Figure 3d, was fabricated with nanoporous platinum electrodes electrodeposited onto openings etched in  $3 \mu\text{m}$  thick parylene-C, which encapsulated 400 nm thick gold interconnects. These parylene cores were then transfer printed onto  $40 \mu\text{m}$  thick collagen substrate and encapsulated with Matrigel. Upon insertion into the motor cortex, the microelectrode softens by hydration, with the Young's modulus of hydrated collagen

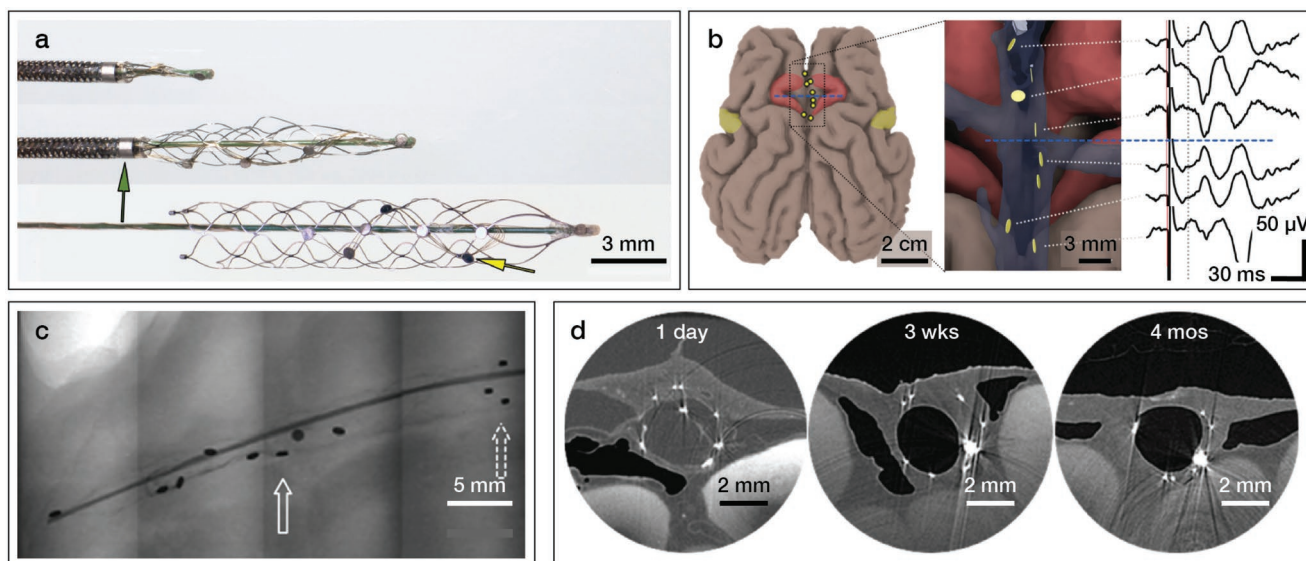


**Figure 5.** A summary of the Stentrode, an endovascular neuroimplantable device for electrophysiological recording from the cortex. a) Self-expanding nitinol stent with platinum electrodes (yellow arrow), deployed from a 4F catheter (green arrow). b) Schematic showing the Stentrode placed in the superior sagittal sinus (SSS) vein and representative electrical recordings from electrodes at different locations. c) Side view of the Stentrode post-implantation. White arrows point to electrodes. d) Progression of the Stentrode's incorporation into SSS vessel wall over a period of four months. Adapted with permission.<sup>[59]</sup> Copyright 2016, Springer Nature.

film at  $\approx 2.64 \pm 1.1$  MPa and of hydrated Matrigel at  $\approx 450$  Pa. Implantation of the ECM-based probe can occur with the same procedure as a silicon-based Michigan probe, since the dehydrated collagen device has a modulus value of  $\approx 3.4$  MPa and a buckling force of  $2.87 \times 10^{-2}$  N, similar to that of a Michigan probe ( $5.42 \times 10^{-2}$  N). To prevent hydration-induced buckling during implantation, an insertion speed of at least  $300 \mu\text{m s}^{-1}$  is required. Histological assays of brain tissue after 16 weeks of implantation (1.2 mm into the rat motor cortex) showed a reduced astrocyte response, less glial scarring, and higher neuronal density at the implantation site when compared to a PDMS-based control microelectrode.

The use of collagen and other biologically available substrate materials with dynamic hydration-based stiffness could lead to more benign neuroimplantable devices that can utilize existing implantation procedures for Si-based probes. However, thinner and longer probe geometries required for deep brain interactions may result in mechanical failure of a biomaterial device via buckling during implantation. Further studies are required to determine the viability of using such materials for chronic *in vivo* studies. Trials of these probes in nonhuman primates are especially necessary for establishing device integrity during the implantation procedure and functionality during chronic placement in the brain. Such demonstrations are crucial in order to proceed to human clinical trials.

### 2.3. Endovascular Probes (Stentrode)

Unlike traditional approaches to cortical surface electrical measurements such as ECoG and shallow multielectrode arrays, stent-based electrodes (Stentrode) query clusters of neurons via electrodes placed inside the brain's vascular network,

most often in the superior sagittal sinus (SSS), a vein which lies in the large sulcal fold running across the center of the brain. The Stentrode is depicted in Figure 2g and shown in Figure 5. The first report of this neuroimplantable device demonstrated a Stentrode implanted in the SSS, adjacent to the motor cortex in the superior frontal gyrus.<sup>[59]</sup> The device consists of platinum 750  $\mu\text{m}$  diameter platinum electrodes welded onto a commercially available nitinol stent and wired with 25  $\mu\text{m}$  diameter platinum-tungsten wires insulated with a 6  $\mu\text{m}$  thick polyimide. The nitinol stent allows for the self-expanding nature of the device, for which it can grow from  $\approx 300 \mu\text{m}$  to 3 mm in diameter. The implantation procedure is minimally invasive, as the entry point at the external jugular vein requires only a cut in the neck and slow guidance of the Stentrode into the target location, where it incorporates into the vessel wall within 7 d. It was able to achieve a 2.4 mm electrode pitch and maintained signal quality for 190 d when chronically implanted into sheep.

The Stentrode, now a trademarked, patented device, has rapidly evolved from its first scientific publication in 2016<sup>[59]</sup> to preparation for pilot clinical trials in 2019.<sup>[89]</sup> Furthermore, the Stentrode has also been shown to provide similar signal quality (bandwidth and signal-to-noise ratio) to conventional epidural and subdural electrodes.<sup>[90,91]</sup> Four factors have likely led to the Stentrode's speedy progression along the FDA approval process: i) its electrode and insulation materials have been widely established in commercial neuroimplantable devices, ii) its technology involves very modest changes to the existing, FDA-approved stent that is commonly used to unclog blood vasculature, iii) its implantation procedure is a slightly modified version of catheter venal angiography, which has also been well established in the medical community for decades, and doctors regularly employ it in nonneurosurgical procedures, and iv) it has been verified through many studies with high sample size

to test the viability,<sup>[59]</sup> functionality,<sup>[91]</sup> and biocompatibility<sup>[59,90]</sup> of the Stentrode. Notably, the background of the team responsible for initial publications on the Stentrode was extremely diverse. Their first paper incorporated author backgrounds from academic medical, physics, aerospace, mechanical, and materials science departments, as well as surgical and veterinary hospitals.<sup>[59]</sup> Including a fusion of clinician, surgeon, veterinarian, and engineering feedback early on in the process of neuroimplantable device development may have had implications for its rapid advancement from bench to clinic.

The Stentrode also holds promise for querying deep brain structures, as the intracranial vascular system reaches the depths of the hippocampus and subthalamic nucleus. Studies are underway to devise inductive and capacitive methods to power intracranial Stentrode wirelessly (near-field radio frequency (RF),  $\approx 30$  mm transmission depth, 500 mW input, 2% transmission efficiency) from outside the cranium.<sup>[92]</sup> Such advancements would make this endovascular neuroimplantable device more promising, as no external, wired power source would need to be installed or replaced, thus decreasing its overall invasiveness and increasing its ease of use during chronic implantation.

## 2.4. Depth Probes

Since their recording abilities limit their interfacing localities primarily to the somatosensory cortex, ECoG arrays and shallow MEAs are often employed for BCIs oriented toward neuroprosthetic applications. Depth probes, however, open up an entirely new arena of subcortical, deep brain structures for neuromodulation. Neuronal querying, drug delivery, and optical modulation of these structures, such as the substantia nigra, amygdala, and hippocampus, may ultimately help enlighten mechanisms for many poorly understood afflictions that potentially have a basis in altered brain tissue or dynamic neuronal genetic expression, such as mood disorders,<sup>[93–95]</sup> anxiety,<sup>[96]</sup> depression,<sup>[96,97]</sup> and Alzheimer's disease.<sup>[98]</sup>

### 2.4.1. FDA-Approved Deep Brain Probes

Development of depth probes for implantation into the human brain began in the mid-20th century in the interest of treating movement-related disorders, e.g. stimulation of the STN for treatment of PD.<sup>[2,103]</sup> The DBS electrode, depicted in Figure 2h and shown in Figure 6b, consists of a flexible 1.27 mm diameter cylinder (coiled wire with polyurethane insulation) with four stacked platinum/iridium cylindrical electrodes of 1 mm height and 0.5–1.0 mm pitch (Medtronic, Inc.). Each active electrode can emit a continuous spherical electric field radiating outward at the stimulation site. Advancements in DBS electrode technology have seen large numbers of electrodes used to emit a directional, rather than uniformly spherical, electric field, as well as electrodes with multiple independent current control (MICC), which allows for unique and simultaneous electrical stimulation at different contacts.<sup>[103]</sup>

To create a closed-loop therapeutic experience for patients with epilepsy, Neuropace has developed a commercially

available technology that combines deep brain stimulation with ECoG to detect shallow cortical neural behavior and respond with asynchronous stimulation. In part due to this device's combination of two long-standing FDA-approved devices, neuropace's responsive neurostimulation (RNS) system was successful in passing clinical trials and is now commercially available.<sup>[17]</sup> Still, the RNS system was required to undergo pre-market approval (PMA),<sup>[17]</sup> which is required for more risky, Class III devices.<sup>[37]</sup> The popularity of DBS techniques has nevertheless expanded quite rapidly, with over 40 brain targets having been identified for treatment of over 30 disorders, including depression, anorexia, and cluster headaches.<sup>[104]</sup>

### 2.4.2. Nonclinically Approved Deep Brain Probes

*Michigan Probe:* The Michigan Probe, depicted in Figure 2i and shown in Figure 6a, is a microelectrode array in which multiple channels are located on a single shank.<sup>[82]</sup> Depending on the depth of targeted neurons, the length of a Michigan electrode can range from 2 to 15 mm. Due to the relatively large length of Michigan probes, and their targeting of deep brain structures, the authors will consider them in this paper to be depth probes. Unlike the Utah MEA, which is fabricated by out-of-plane processes, Michigan-style microelectrodes are well-known examples of neuroimplantable devices manufactured by in-plane approaches. The typical microfabrication process flow includes a boron doping process to define the profile and thickness of the shank, a metal coating deposition on the bottom insulating layer, and subsequent patterning to form recording sites, interconnecting traces, and bonding pads via photolithographic techniques.<sup>[105]</sup> The top insulating layer is then deposited, followed by exposing of the recording and bonding pads via photolithographic techniques and etching processes. Eventually, an anisotropic etching is carried out to release the electrode using ethylene diamine pyrocatechol (EDP), as boron doped p-type Si has slower etching rate than that of undoped Si. Still, multiple planar Michigan electrodes also can be electrically packaged into a 3D array layout.

One benefit of the in-plane microfabrication process is that it allows monolithic integration of the microelectrode with signal processing circuitry that filters, amplifies, multiplexes and digitizes the spike signals from neurons. Additionally, unlike Utah MEAs and microwire electrode arrays, the increase in the number of recording sites for Michigan probes does not significantly enlarge the footprint of the entire microsystem. It is also feasible to create an innovative microelectrode with a high density of recording sites to better decode a wide range of human brain activity. It was reported that a novel Michigan-style probe, the NeuroPixels probe, arranged 384 recording channels and 960 titanium nitride recording sites ( $20 \mu\text{m} \times 20 \mu\text{m}$ ) on an extremely thin needle shank (10 mm long,  $20 \mu\text{m}$  thick, and  $70 \mu\text{m}$  wide).<sup>[60]</sup> The NeuroPixels probe is available for purchase by the research community for use in preclinical trials. Research generated by this probe from research groups around the world could be a path toward a clinical application.

In a separate case, Michigan electrodes were found to consistently and reliably provide high-quality spike recordings over extended periods of time lasting up to 127 d with 13/14 (93%)

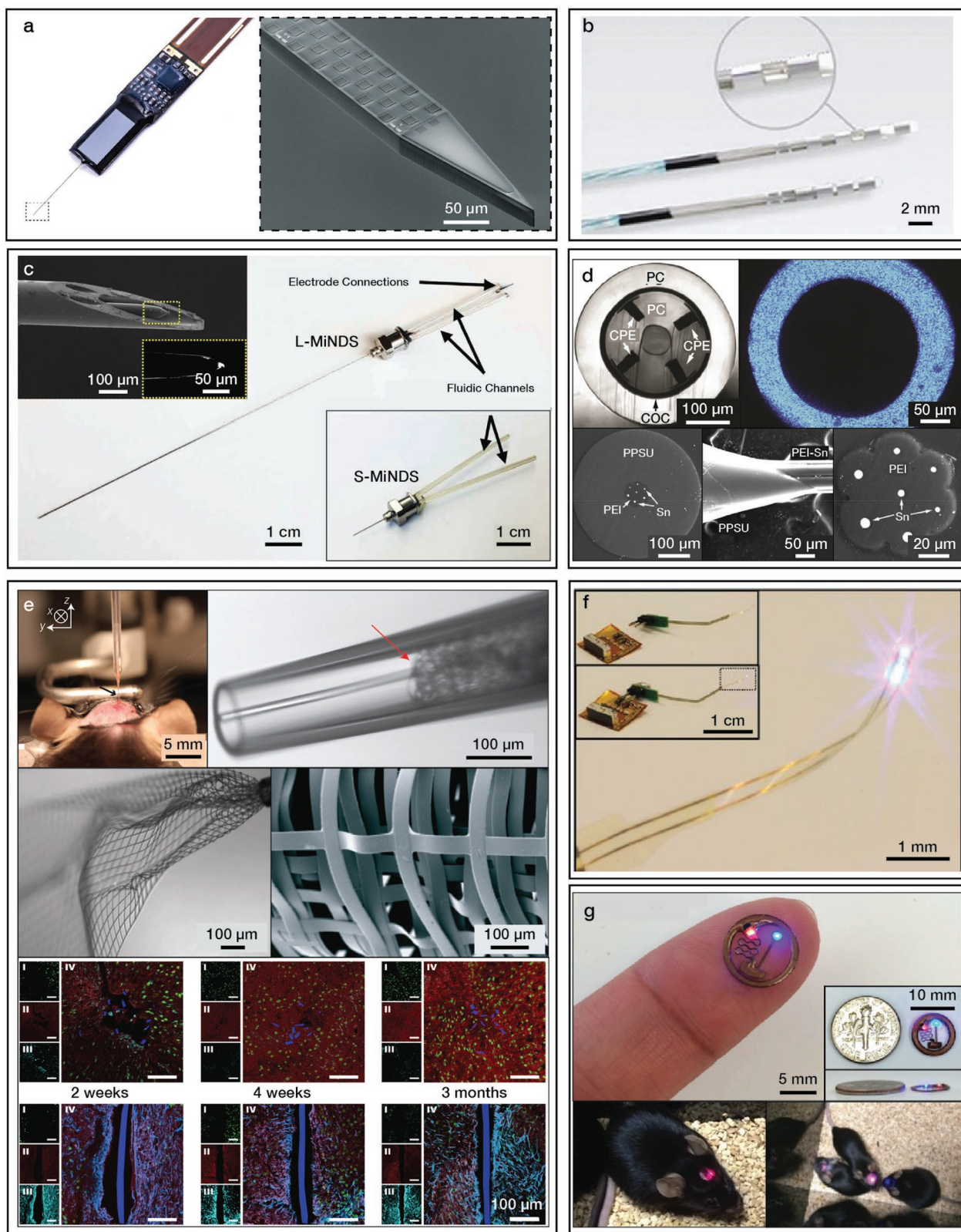


**Figure 6.** A summary of depth probes representing various form factors, functionalities, and material choices. a) Michigan-style NeuroPixels probe. Inset shows zoomed-in tip of the NeuroPixels probe, with checkered TiN electrodes on a silicon substrate. Adapted with permission.<sup>[99]</sup> Copyright 2019, Interuniversitair Micro-Electronica Centrum (IMEC). b) Deep brain stimulation probe available from Abbott. Circular inset shows close-up of directional leads. Adapted under the terms of the CC-BY license.<sup>[100]</sup> Copyright 2018, the Authors. Published by Frontiers Media SA. c) Miniaturized

of the devices remaining functional in ten rodents throughout the assessment period.<sup>[106]</sup> In addition, rabbit and nonhuman primate models have been implanted to test surgical techniques and in vivo functionality.<sup>[107]</sup> The recorded electrophysiological signals showed high signal-to-noise ratios for periods extending beyond one month. Although the limited thickness of Michigan probes reduces tissue damage during implantation, their rigid, fragile geometry based on silicon substrates combined with their increased length brings new challenges of avoiding mechanical failure during the surgical insertion process.

*Conformable, Localized Deep Brain Drug Delivery:* Since administering a drug-based therapeutic intervention, such as Levodopa for PD, results in broad, unlocalized effects on the brain, DBS does provide a unique alternative due to its localized delivery of treatment, i.e., electrical pulses, at the location of interest. However, continuous electrical pulses provided at a large group of neurons (several cubic millimeter volume) can cause patient-dependent complications with speech, swallowing, cognition, and mood due to relatively unlocalized stimulation.<sup>[103]</sup> A potential alternative arises from a depth probe that bypasses the blood–brain barrier (BBB) and delivers drugs to subcubic millimeter volumes in the brain with sub-microliter resolution. One recent example of such a device is the miniaturized neural drug delivery system (MiNDS), depicted in Figure 2j as well as in Figure 6c. It consists of a 75  $\mu\text{m}$  diameter tungsten electrode for assessing neuronal activity at the drug delivery site, two 30  $\mu\text{m}$  outer diameter, 5  $\mu\text{m}$  wall thickness borosilicate channels for drug delivery, and a 9  $\mu\text{m}$  thick polyimide backing all aligned inside a 200  $\mu\text{m}$  outer diameter, 25  $\mu\text{m}$  wall thickness etched stainless steel Hamilton needle.<sup>[6]</sup> Histological assays of neuronal tissue at the implant site after chronic implantation of MiNDS in mice for eight weeks show that cell death and glial response are limited to the tissue within a 500  $\mu\text{m}$  radius around the implant. MiNDS is mostly comprised of materials (tungsten, polyimide, and stainless steel) which have been empirically used in chronic neural implants since the 1970s and which have been approved in several BCIs by the FDA. In addition, the device has an areal footprint less than 5% that of commercially available DBS electrodes by Medtronic, Inc. MiNDS, therefore, exemplifies a neuroimplantable device that could make a faster, smoother transition from the research phase to clinical trials.

In a similar device, created ten years prior, which lacked in vivo trials, researchers designed flexible microfluidic channels and electrodes fabricated on parylene-C substrates to deliver water-soluble drugs in an active manner and PLGA nanoparticles loaded with DEX in a passive manner. The device was also meant to take electrophysiological recordings of neural tissue while simultaneously delivering drugs.<sup>[108]</sup> Unlike the therapeutic drug delivery targeted by MiNDS, however, the purpose of this style of drug delivery is to alter the neural environment immediately surrounding the probe so as to reduce the inflammatory foreign-body response associated with puncturing of the brain tissue. Furthermore, although the intent of drug delivery was motivated by valid concerns of foreign body response, the use of encapsulated microfluidic channels to deliver drugs only secreted drugs at specific points near the tip of the probe, whereas tissue scarring occurred along the entire length of the implanted probe. Congruently, recent progress in therapeutic drug delivery has attempted to use conductive polymers, but a functional in vivo demonstration has yet to be realized due to difficulty sustaining therapeutic levels of drugs and overcoming the in vivo scar-tissue reaction.<sup>[109]</sup> The lack of in vivo trials also lessens the impact of innovations in neural interfacing. Future work in neuroimplantable devices for simultaneous drug delivery and electrical recording may focus on conducting rigorous in vivo trials in rodents and nonhuman primates in order to work toward FDA clearance for clinical trials.

*Syringe-Injectable Neural Interfaces:* A novel form factor for accessing deep brain structures involves implanting an ultrathin, mesh-like grid of electrodes into deep brain structures via a syringe. Using lift-off microfabrication techniques, researchers have created macroporous mesh nanoelectronic scaffolds made of silicon nanowires with nickel electrodes and Cr/Pd/Cr interconnects, all encapsulated with SU-8 epoxy,<sup>[110]</sup> a biocompatible material commonly used in medical implants. Each of the polymeric ribbons making up the mesh is between 10–40  $\mu\text{m}$  in width, and the final device thickness is less than one micron. These scaffolds were further shown to incorporate well with collagen, Matrigel, and PLGA to create hybrid bioelectronic interfaces upon which embryonic rat hippocampal cells were successfully cultured for up to three weeks.

A follow-up study altered material composition of the mesh electronics and utilized materials more commonly used in

---

neural drug delivery system (MiNDS). Depth probe for simultaneous drug delivery with nanoliter precision and electrical recording with pinpoint micrometer-scale accuracy. Image shows L-MiNDS, or long MiNDS, with 10 cm needle length. Bottom right inset shows S-MiNDS, or small MiNDS, with 1 cm needle length. Top left inset shows SEM image of MiNDS tip with drug infusion channels and electrode tip further zoomed in. Adapted with permission.<sup>[6]</sup> Copyright 2018, AAAS. d) Thermally drawn, polymer-based probes. From left to right, top to bottom: distal end view of multimodal probe for simultaneous drug delivery, electrophysiological recording, and optogenetic modulation; light profile of multimodal probe; multielectrode probe with sacrificial polyphenylsulfone (PPSU) layer after first thermal drawing process; PPSU layer removed during second thermal drawing process; final multielectrode probe after fabrication. Adapted with permission.<sup>[63]</sup> Copyright 2015, Springer Nature. e) Syringe-injectable mesh electronics. From left to right, top to bottom: implantation of mesh electronics with glass syringe; mesh electronics inside tip of syringe, where the red arrow indicates the end of mesh electronics within the syringe; mesh electronics ejected from syringe; SEM image of mesh electronics; biocompatibility tests of syringe-injectable electronics compared to a thin film probe show tissue healing and seamless integration of neural tissue with mesh electronics (all scale bars are 100  $\mu\text{m}$ ). Adapted with permission.<sup>[61]</sup> Copyright 2015, Springer Nature. Adapted under the terms of the CC-BY license.<sup>[101]</sup> Copyright 2017, the Authors. Published by PNAS. f) First in vivo wireless depth probe for optogenetic modulation. This polymer-based, wireless, multimodal depth probe can conduct simultaneous electrophysiological recording, temperature sensing, and optogenetic modulation. Adapted with permission.<sup>[102]</sup> Copyright 2013, Springer Nature. g) Near-field wireless optoelectronics. From left to right, top to bottom: size of optoelectronics probe compared to human finger, inset shows size and thickness comparison to United States dime; mouse with wireless optoelectronics seamlessly hidden under the scalp, red light indicates device functionality; wireless functionality allows for studies with multiple subjects for novel social dynamics experiments. Adapted with permission.<sup>[62]</sup> Copyright 2017, Elsevier.

FDA-approved neuroimplantable devices. In these meshes, platinum electrodes (20  $\mu\text{m}$  diameter and 50 nm thick) and Cr/Au interconnects (2–10  $\mu\text{m}$  wide and 5/100 nm thick), and SU-8 polymer ribbons (5–20  $\mu\text{m}$  wide and 350–400 nm thick) were used.<sup>[61]</sup> These sub-micrometer thick, centimeter-scale mesh electronics, depicted in Figure 2k and shown in Figure 6e, were later shown to successfully laminate to the interior of the brain by uptake through a 100–200  $\mu\text{m}$  inner diameter glass needle syringe and subsequent delivery to deep brain structures such as the hippocampus and the lateral ventricle. Acute in vivo trials were conducted in a rat model using a 16-channel mesh electrode and five-week chronic histology assays revealed greater biocompatibility compared to a control of the same thickness as the mesh electronics but with a standard thin film form factor, likely due to ultralow bending stiffness (0.087  $\text{nN m}^{-1}$ ) and feature sizes on the order of single neuron dimensions. During chronic implantation of mesh electronics, tissue healing was observed four weeks after initial scarring by the syringe and after three months, the mesh electronics seamlessly integrated with surrounding neural tissue, with little to no remaining immunological response. Neurons were found to penetrate through the macroporous mesh structure, demonstrating unprecedented levels of tissue integration in neural probes.<sup>[101]</sup>

Despite the reduced foreign body response, syringe-injectable mesh electronics are susceptible to buckling and crumpling during insertion, which lead to lower accuracy of device implantation in the specific target region of interest and reduced time of device functionality, but this issue can be partially abetted by using a motorized control stage of the rate of syringe withdrawal.<sup>[111]</sup> Syringe-injectable mesh electronics present a promising next-generation form factor with remarkably high rates of biological integration. Likely due to the complicated, high precision, and motorized implantation procedure that has not been used for FDA predicates, no current variations of this technology is currently in clinical trials. An implantation method that matches those used for common neural surgeries or for implantation of commercially available neuroimplantable devices would possibly push these mesh electronics closer to FDA clearance.

*Deep Brain, Multimodal Optogenetic Probes:* While syringe-injectable mesh electronics present a novel form factor for electrical querying of deep brain structures, optogenetic probes present an alternative modality for achieving the functionality of neuromodulation, including stimulation and inhibition. These probes allow for high spatiotemporal resolutions such that single neurons altered to express the light-sensitive opsin channelrhodopsin-2 (ChR2) can be controlled by optical modulation of blue light (450–490 nm).<sup>[112]</sup> Since the first proof-of-concept in vitro study conducted on rat hippocampal neurons in 2005,<sup>[34]</sup> in vivo optogenetic neuromodulation has been enabled by advancements in microfabrication techniques for optical components such as micro-LEDs and waveguides.

Many of the neuroimplantable devices implementing optogenetic control in deep brain structures also tend to incorporate other functionalities, such as electrophysiological recording for neural probing during photonic stimulation.<sup>[113]</sup> The first in vivo trial of a multimodal optogenetic neuroimplantable

device incorporated an SU-8 waveguide coated with 200 nm gold, tungsten–titanium metal cladding, microfluidic channels for drug delivery, and electrodes on a polyimide–platinum–polyimide (5–0.3–5  $\mu\text{m}$  thick) substrate shaft.<sup>[114]</sup> The study demonstrated the viability of microfabricated optoelectronic neuroimplantable devices to manipulate behavior of inhibitory neurons in the rodent hippocampus.<sup>[114]</sup> In another study, researchers created a quad-shank neural probe in which each shank consisted of a 15  $\mu\text{m}$  thick, 30  $\mu\text{m}$  wide SU-8 waveguide on a 20  $\mu\text{m}$  thick, 30  $\mu\text{m}$  wide glass cladding layer embedded in a 30  $\mu\text{m}$  thick, 86  $\mu\text{m}$  wide silicon-on-oxide (SOI) substrate.<sup>[115]</sup> The shanks, ranging from 3–6 mm length, each included eight iridium contacts, with area  $14 \times 14 \mu\text{m}$ , for simultaneous electrical recording. The use of four shanks with different lengths allows for neuromodulation in different locations within one animal. This form factor enabled researchers to target early stopping of seizure progression across neural tissue in different areas of the brain.

Another device, depicted in Figure 2m and shown in Figure 6d, incorporating multimodal functionality (optical stimulation, electrical recording, and drug delivery) was created in a novel, flexible form factor—a 200  $\mu\text{m}$  diameter fiber without the need for microfabrication.<sup>[63]</sup> The fabrication procedure involves a thermal drawing process (TDP) using polymer, metal, and composite materials. A macroscale preform of the fiber is repeatedly heated and stretched into a fiber. Materials commonly used in medical devices, including polycarbonate (PC), conductive polyethylene (CPE), and cyclic olefin copolymer (COC), were selected for use in these preforms. Another 85  $\mu\text{m}$  diameter TDP-based fiber for electrical recording purposes was constructed with poly(etherimide) (PEI) for insulation and tin (Sn) for electrical contacts. The TDP process necessitates that materials used in the same preform must possess similar glass transition temperatures and melting temperatures, so care was taken to choose functional materials of similar thermal properties, as well. The device demonstrated chronic viability in an in vivo rodent model for two months. One drawback of the TDP-fabricated functional neural fiber is that its active sites all lie at the very distal area, limiting interaction with neuronal populations to a single site. Nevertheless, fibrous, flexible form factors represent novel explorations of different fabrication techniques like TDP that are viable for the scalable mass manufacturing of neuroimplantable devices. These explorations are necessary for early-stage academic research focused on creating new technologies, but would likely take an extended period of time to progress through the FDA approval process and reach the market.

*Deep Brain, Wireless Multimodal Optogenetic Probes:* Due partially to the promise of in vivo optogenetic research to uncover neural circuits with high spatiotemporal resolution, the field has naturally gravitated toward fully wireless modulation and measurement for acceleration of these technologies toward clinical applications. The first such device is an RF-based wireless, flexible, multimodal depth probe capable of simultaneous electrophysiological recording, temperature sensing, and optical modulation of neurons.<sup>[102]</sup> The multifunctional system, shown in Figure 6f, consists of four different active layers: i) a 20  $\mu\text{m} \times 20 \mu\text{m}$  Pt electrode for electrical recording or stimulation, ii) a microscale inorganic photodetector ( $\mu\text{-IPD}$ ), which

is a 1.25  $\mu\text{m}$  thick, 200  $\mu\text{m} \times 200 \mu\text{m}$  silicon photodiode, iii) four microscale inorganic LED's connected in parallel, and iv) a Pt serpentine resistor used as a precision temperature sensor or heater. The layers are attached to each other using 500 nm thick layers of epoxy. These layers are attached with a bioresorbable adhesive based on purified silk fibroin, which allows for removal of the microneedle after implantation of the depth probe. This microfabricated RF-based optogenetics device and its successful operation for up to four weeks represent a novel stride into closed-loop wireless optogenetic modulation for expediting the adoption of optogenetics technologies in clinical applications.

To improve further upon wireless optogenetics, researchers have even progressed to create a fully near-field wireless, flexible optoelectronic neuroimplantable device that can be hidden subdermally after implantation.<sup>[62]</sup> The device, depicted in Figure 2l and shown in Figure 6g, consists of a flexible near-field communication (NFC) coil connected by serpentine interconnects to a 80–130  $\mu\text{m}$  thick  $\times$  350  $\mu\text{m}$  wide injectable needle, which has a microscale inorganic LED ( $\mu$ -ILED, 270  $\mu\text{m} \times 220 \mu\text{m} \times 50 \mu\text{m}$ ) at the tip for optical stimulation. Importantly, the serpentine interconnects allow for independent movement of the probe tip and the NFC coil, so as to minimize internal micro-motion-related scarring with rodent movement during in vivo trials. The NFC coil consisted of thin film copper, 5  $\mu\text{m}$  thick parylene-C and 0.5–300  $\mu\text{m}$  thick PDMS barrier layers, and surface-mount chips and another  $\mu$ -ILED for status indication, all on a flexible 75  $\mu\text{m}$  thick polyimide substrate. The device was chronically implanted in mice for eight weeks, and in vivo studies demonstrate the ability to provide wireless stimulation to dopaminergic neurons in the nucleus accumbens and ventral tegmental area for promotion of reward-based reinforcement behaviors.

One advantage of creating such fully wireless neuroimplantable devices is that they allow for new types of scientific experiments. For example, the battery-free, untethered, lightweight device described above can be used to observe the behavior of multiple animals at once. Another study demonstrated that such wireless optogenetic devices can also interface with the motor cortex, spinal cord, and peripheral nerves in the arms and legs in in vivo rodent models.<sup>[116]</sup> Despite these devices' use of copper, which is not biocompatible with bodily tissue, the double insulation in parylene-C and polyimide ensures that no interaction between bodily tissue and the NFC coil can occur. Such nonporous insulation is critical for chronic neural interfacing—especially for conformable, wireless neuroimplantable devices that use potentially harmful materials such as copper—so as to prevent toxic biological reactions and device damage in vivo.

## 2.5. Neural Dust

In the same vein of research efforts, a wireless neuroimplantable device that blends in seamlessly with brain tissue has been pursued in research for several years now. As a step toward realizing that goal, neural dust proposes an ultrasonic backscatter wireless paradigm for electrophysiological recording of nervous tissue. Ultrasonic energy is safe for use in the body at

most frequencies and power levels, and it has medical precedents. So far, neural dust has only been demonstrated in vivo in the peripheral nervous system, specifically the sciatic nerve, in a millimeter-scale device.<sup>[46,117]</sup> The neural dust “mote” consists of a 50  $\mu\text{m}$  thick polyimide flexible printed circuit board upon which a piezocrystal and custom transistor are attached using conductive silver paste to aluminum wirebonds and conductive gold traces (Figure 7).<sup>[28]</sup>

Ultrasonic energy attenuates less than electromagnetic (EM) radiation in tissue;<sup>[28]</sup> however, the cranial bone dampens ultrasonic waves considerably through absorption, reflection, scattering, and mode conversion.<sup>[119]</sup> Furthermore, since the acoustic domain typically operates in lower frequencies than the EM domain, and because sound travels slower than light, bulkier materials are required to resonate at ultrasonic frequencies. Shrinking the piezocrystal would, therefore, degrade the signal-to-noise ratio of the backscatter link.<sup>[117]</sup> While neural dust provides a step toward a desirable form factor, much work remains to be done to achieve further miniaturization of a wireless neuroimplantable device that can accomplish transcranial communication and power transfer at safe energy levels.

## 3. Implantation-Related Risk Factors

As covered in Section 2, many of the functional properties and risk factors associated with neuroimplantable devices stem from material selections and form factor.<sup>[120]</sup> However, the surgical protocols and methods for implantation, i.e., the implantation procedure, have been shown to greatly contribute to clinical safety concerns,<sup>[121,122]</sup> fidelity of interfacing,<sup>[123]</sup> and efficacy of treatment.<sup>[123]</sup>

Historically, the implantation of neural probes—including epicortical systems like ECoG, intracortical systems like the Utah array, and deep brain systems like DBS—have required the use of stereotactic craniotomy. In this procedure, the patient remains fully awake under an anesthetic such as propofol, and motor responses from the patient are used to guide the probes to their target locations.<sup>[124]</sup> Inherently, a portion of the skull is extracted to permit the insertion of probes. However, the exposure of the meningeal layers to the outside environment and to medical instruments results in increased risk of bacterial infections. A study by Kourbeti et al. (2015) found that the main infection-associated risk factors during the implantation process were meningitis (4.8% of cases) and gram negative bacteria such as *Acinetobacter* and *Klebsiella* spp. (44% of cases).<sup>[125]</sup> Additionally, ventilator-associated pneumonia was the most common infection in the study population. Implicitly, an open skull craniotomy is a factor that renders traditional neuroimplantable devices disadvantageous compared to novel devices discussed in Section 2.

An important paradox arises for neuroimplantable probes requiring traditional implantation procedures. Since implantation for neural interfacing often requires the use of stiff materials with high Young's modulus, the issue of mechanical mismatch with neural tissue is difficult to avoid. Specifically, the viscoelastic and inhomogeneous properties of the neural tissue make the mechanics of probe insertion a complex process, in which device materials, dimensions, stiffness,

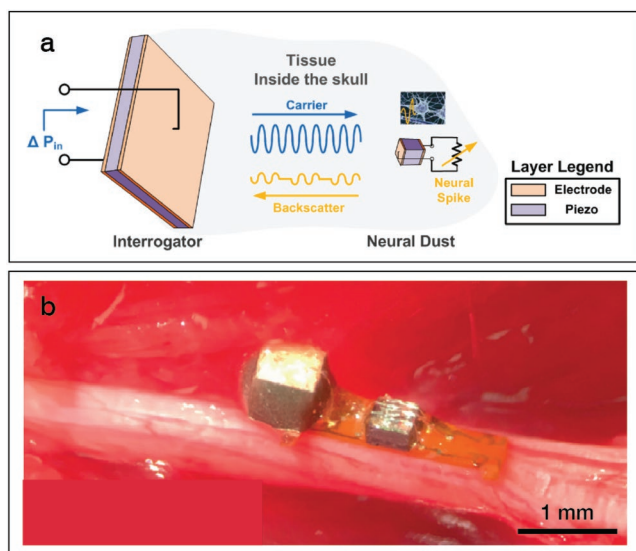


**Figure 7.** A summary of neural dust. a) Conceptual explanation of ultrasonic backscatter mechanism for wireless transmission of electrophysiological recordings taken in vivo, by which a piezocrystal modulates the backscattered signal sent to a receiver outside the brain. Adapted with permission.<sup>[118]</sup> Copyright 2018, M. Maharbiz. b) Neural dust mote shown on the sciatic nerve in vivo. Adapted with permission.<sup>[28]</sup> Copyright 2016, Elsevier.

sharpness, and target location in the brain must be carefully considered.<sup>[126]</sup> For example, as evidenced by the use of collagen for substrate material, as discussed in Section 2.2.2, materials with a low Young's modulus cannot be implanted without the help of a stiff backing or dynamic altering of stiffness.<sup>[58]</sup> Just as a flexible material like polyimide cannot penetrate a jelly-like substance as easily or as precisely as a needle, so too do neuroimplantable devices based on highly flexible materials or biomaterials require temporary stiffening during implantation. This dynamic stiffness can be achieved by using materials that naturally change stiffness when transitioning from dehydrated to hydrated conditions—such as collagen,<sup>[58]</sup> poly(vinyl acetate) (PVAc),<sup>[127]</sup> PEG,<sup>[128]</sup> silk,<sup>[129]</sup> carboxy-methylcellulose,<sup>[130]</sup> and sucrose gel<sup>[131]</sup>—or upon removal of a temporary, pressurized liquid stiffening agent such as gallium.<sup>[132]</sup> Besides designing probes with materials of tunable stiffness, another method for implantation of flexible probes utilizes a stiff “shuttle” for delivery of the probe to the target location. This stiff shuttle can either be removed immediately after implantation<sup>[26]</sup> or, if bioresorbable materials are used, can dissolve seamlessly into neural tissue with time.<sup>[51,133–135]</sup> Materials engineering, and especially the implementation of dynamic stiffness during implantation, is necessary for creating new interfaces that can achieve both reliable implantation and improved biocompatibility.

Generally, new developments in probe architecture and delivery mechanisms have permitted less invasive modes of implantation, reducing potential factors that could lead to infection. Stentrode delivery, as mentioned in Section 2.3, has provided one avenue for transcranial recording without the need for a craniotomy, since implantation involves a catheter-based venography started in the jugular vein and guided into cerebral veins.<sup>[59]</sup> Additionally, syringe-injectable mesh electronics, detailed in Section 2.4.2, can be implanted with a less invasive

transcranial procedure, through the use of a hypodermic needle, loaded with the mesh. After injection of the mesh into the target area of brain, the needle is removed, and tissue analysis indicates healing over time.<sup>[101,136]</sup> Others have further speculated whether a structurally analogous mesh can be injected intravenously, but in a region outside of the brain's vasculature.<sup>[137]</sup> Such a method, if possible, would reduce exposure of the meningeal layers to the outside environment, lessening the risk of infection or scarring.<sup>[138]</sup> New wireless modalities such as neural dust, as described in Section 2.5, if further miniaturized and implanted in the central nervous system, have the potential to further reduce implantation-related acute risk factors by bypassing conventional stereotactic open-brain surgery altogether.<sup>[117]</sup> Thereby, novel form factors—such as syringe-injectable mesh electronics, Stentrode, and neural dust—and novel functionalities such as wireless communication, de-risk not only the downstream consequences of mechanical mismatch and chronic usage, but also those associated with the acute procedure of placement.

Following implantation, the stability of neural devices depends on risk factors related to mechanical device design<sup>[46,47,139]</sup> and biological foreign-body response.<sup>[46,80,140,141]</sup> As examined in Section 5.2, neural probe failure is most often mechanical in nature, whether as a result of interconnect failure,<sup>[139]</sup> cracking or breach of the encapsulation,<sup>[46,142]</sup> or electrode corrosion.<sup>[143]</sup> Such failures are the primary cause of FDA recalls for neuroimplantable devices, as discussed in Section 5.3. More detailed information on mechanical failure modes of neural probes can be found in relevant literature.<sup>[46,139,140]</sup> Biological failure modes, such as BBB breach,<sup>[144]</sup> glial scarring,<sup>[49,80,140,145]</sup> and tissue micromotion,<sup>[49]</sup> are discussed in detail in Section 4.

## 4. Biological Risk Factors Inherent to Regions of the Brain

Material selection, functionality, form factor, and implantation procedure have strong implications for the long-term use of neuroimplantable devices in biological tissue. Due to the intrinsic heterogeneity of the brain, risk factors for infection vary based on the type of device as well as the region of the brain that undergoes physical disruption as a result of implantation. The range of acute adverse effects related to the implantation of neural probes consists of infections, disruption of blood and CSF circulation, and tissue scarring.<sup>[139]</sup> Each layer of the human central nervous system presents unique considerations for engineering biocompatible materials in order to create conformable neuroimplantable devices.

**Figure 8** illustrates the relevant layers of brain tissue, the placement electrodes at varying depths, and local biological risk factors for each region. Different probe types—such as MEAs, ECoG systems, and depth electrodes—as well as their materials present unique challenges to the development of devices with low failure rates and long operating lifetimes.

### 4.1. Meningeal Risk Factors

All penetrating electrodes are implanted to record from areas in the cortex or the deep brain, which requires puncturing of

the meningeal layers. The meninges are three membrane-rich layers just below the surface of the skull, known as the dura, the arachnoid, and the pia layers.

The uppermost meningeal region is the dense and fibrous dura mater. Biological risks in this area can be classified into three major categories. Firstly, acute penetration of neural tissue can result in trauma, including epidural hematoma and cerebral edema.<sup>[150]</sup> Secondly, there is a risk of direct infection of the dura, typically involving skin pathogens such as *Staphylococcus aureus* and *Staphylococcus epidermidis*.<sup>[151]</sup> Thirdly, probes may be subject to direct cellular encapsulation, which results in lower SNR, dampening electrical signals to and from the probe.<sup>[139]</sup> Finally, chronic implantation of neural probes cascades an inflammatory response resulting in microglial and astrocytic agglomeration, common to all of the meningeal layers. This inflammatory response

is often exacerbated by the presence of rigid metallic probe materials such as silicon and tungsten ( $\approx 100$  GPa), which are stiffer than brain tissue ( $\approx 1$  kPa) by seven orders of magnitude.<sup>[140]</sup> The issue of mechanical mismatch between neuroimplantable devices and neural tissue, therefore, causes a host of issues. As discussed in Sections 2, 3, 4, the use of low-modulus materials or materials with dynamic stiffness for use as substrates in neuroimplantable devices could ameliorate the negative biological effects of chronic neural probe implantation. Furthermore, these materials could be used to create conformable or mesh-like form factors that improve biocompatibility.

Below the dura mater is the arachnoid mater, characterized by a fine and brittle web-like morphology. Here, a major risk factor includes meningitis, which is common to both the arachnoid mater and the pia mater. Additionally, the major CSF

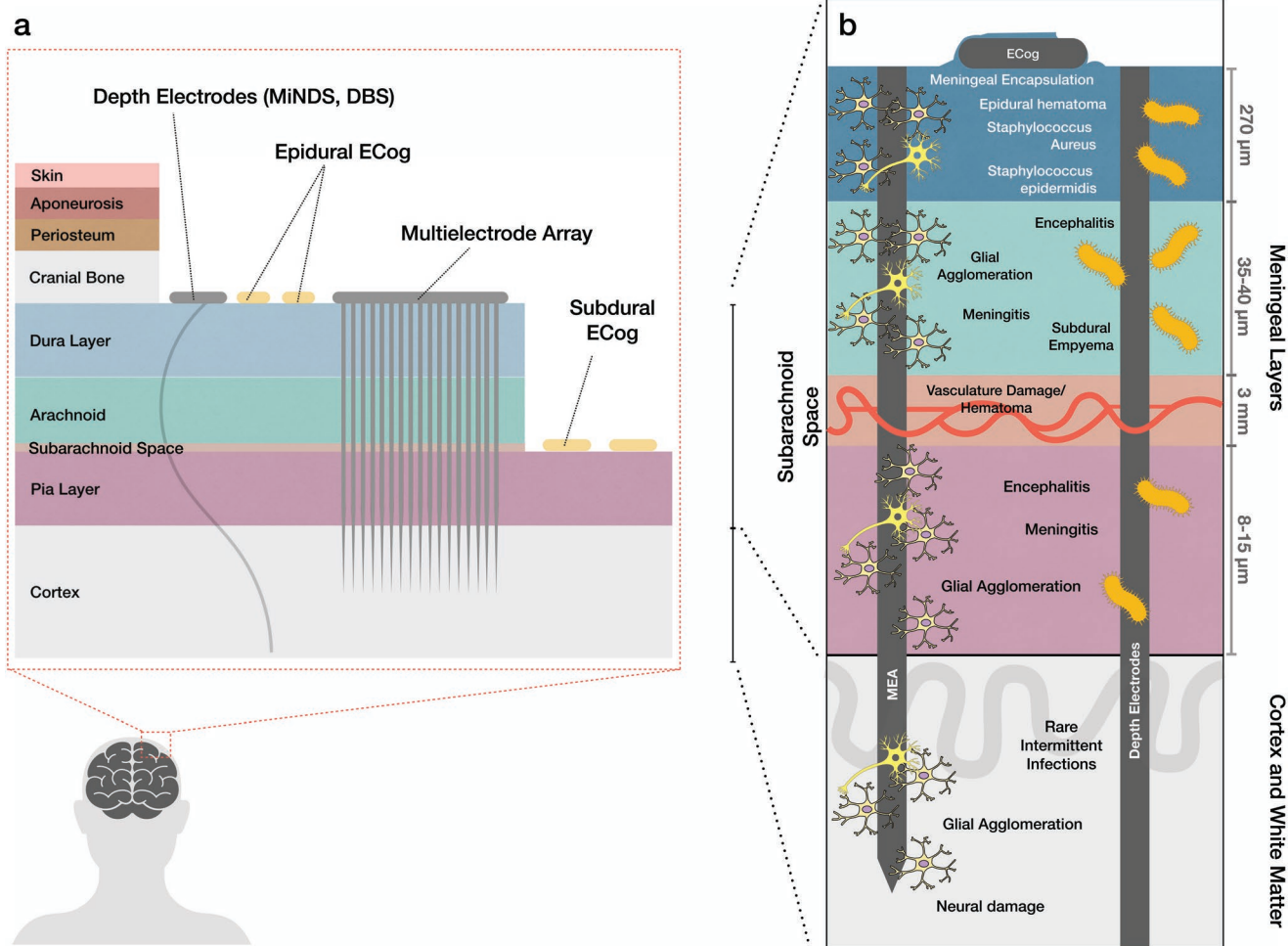


**Figure 8.** A depiction of surface brain layers showing probe placement and risk factors associated with each region. a) A cross sectional diagram of the human scalp, skull, meninges (including the dura, arachnoid, and pia layers), and cortex. Different systems for invasive neural interfacing are shown including epidural/subdural ECog, a multielectrode array (Utah, Michigan, Microwire), and depth electrodes (DBS and MiNDS). b) A diagram of generalized biological risk factors shown for each layer of the meninges and for the human cortical tissue. As shown, infections occur primarily in the meninges with common skin infections being prevalent in the dura layer,<sup>[146]</sup> generalized encephalitis and meningitis occurring in the arachnoid and pia layers,<sup>[147]</sup> and only rare intermittent infections occurring within the cortex.<sup>[148]</sup> Damage to vasculature is primarily regionalized to the subarachnoid space while damage to neurons occurs in the cortex.<sup>[139]</sup> Inflammation and agglomeration of microglia and astrocytes occurs in meningeal as well as cortical layers.<sup>[149]</sup> Dampening of electrical output through meningeal encapsulation of the probes occurs primarily in the dura mater.<sup>[139]</sup> Figure not to scale.

and blood vasculature is primarily localized in the subarachnoid space,<sup>[139]</sup> which can be punctured during implantation due to the use of sharp, high aspect ratio probes such as MEAs and depth probes. This results in a number of failure cases including CSF leaking, hemorrhaging, and hematoma.<sup>[150]</sup> One study found that, in the case of rigid multielectrode arrays, analysis of 60% of the electrode needles showed signs of hemorrhaging after short term implantation due to initial trauma of probe penetration through the brain vasculature.<sup>[140]</sup>

The region of the meninges closest to the cortex is the thin and delicate pia mater. Infection of the pia layer resulting in inflammatory reactions, such as meningitis, is common, as is encephalitis.<sup>[139]</sup> In addition, penetration and tearing of the pia during implantation has been shown to result in increased risk for intracerebral infection.<sup>[152]</sup> Novel form factors and materials for miniaturized, next-generation neuroimplantable devices have reduced the inherent risk to the meningeal layers, since smaller feature sizes minimize of tearing and puncturing of tissue, as discussed in Section 4.3.

#### 4.2. Intracerebral Risk Factors

Intracerebral infections of the brain, which include both grey matter infections and those in deep brain regions, are exceedingly rare, though they should be taken into consideration when making design judgments with regards to DBS and other deep brain implants.<sup>[148]</sup> Most of the case studies on infection factors in the deep brain are concerned with bacterial infections due to poorly sterilized probes<sup>[148]</sup> or puncturing of the pia mater.<sup>[152]</sup> More important to the inherent risks of deep brain implantation is the migration of probes from their target sites, with an average distance of migration of 0.4 mm.<sup>[153]</sup> In one study, postoperative follow-up analyses of migration determined that approximately 12% of patients had leads which migrated more than 3 mm from their implantation sites, resulting in complications such as reduced stimulation efficacy.<sup>[153]</sup> Furthermore, neural damage due to implantation-related trauma, as discussed in Section 3, and rigidity of probe forms, as discussed in Section 2, is an additional issue.<sup>[140]</sup> It is possible that improved material properties for lead fixation at the target site—including rigid nanostructures,<sup>[154]</sup> reinforced silk scaffolds,<sup>[129,155]</sup> and hydration-dependent stiffness<sup>[52,58,127,128,130,131]</sup>—may help to reduce such risks.

#### 4.3. Biological Risk Factors in Relation to Probe Type, Form Factor, and Material Selection

The risk factors described in Sections 5.1 and 5.2 are directly related to the design and fabrication of devices such as silicon microelectrode arrays, Stentrode, and depth systems such as DBS and MiNDS, intended for chronic use.

Due to their planar and flexible form factor, ECoG arrays, which are implanted subdurally or epidurally, do not penetrate the cortex and, therefore, generally avoid disruption to cerebrospinal fluid and intracranial arteries. These devices have been shown to result in less inflammation than electrodes with that penetrate neural tissue.<sup>[146]</sup> Additionally,

relatively few cytological changes consistent with an inflammatory response are seen in ECoG arrays in the dura and pia maters.<sup>[146]</sup> Though dural thickening and fibral encapsulation has been observed in nonhuman primates for epidural ECoG arrays, this does not significantly inhibit long term recording.<sup>[146]</sup> A further study concluded that out of 200 cases of ECoG uses in human subjects, only two faced complications related to surgery and only eight patients experienced perioperative complications such as hardware-related infections and hematomas.<sup>[22]</sup>

Penetrating electrodes such as microwires and silicon-based arrays, due to their often rigid materials choices and sharp form factors, are known to cause increased accumulation of microglia and astrocytes around the implantation site,<sup>[140]</sup> continual local inflammation,<sup>[156]</sup> and progressive local neuronal degeneration.<sup>[157]</sup> Additionally, this risk factor causes the decline of the signal-to-noise ratio of the probe's electrical output.<sup>[12,158–160]</sup> A ten-year study conducted at the University of Oslo found approximately a 5% infection rate after DBS implantation, most of which were associated with skin bacteria such as *S. aureus* and *S. epidermidis*. Most of these cases were linked to implantation or replacement procedures of the implanted pulse generator rather than the chronic duration of intracranial placement.<sup>[151]</sup> Though novel interfacing tools often have less longitudinal health data, they offer hypothetical advantages over the existing state-of-the-art. For instance, advances in the development of Stentrode implants have mitigated chronic local inflammation of neural tissue by avoiding direct contact with cortical neurons and instead targeting neural vasculature.<sup>[59]</sup> Injectable mesh electronics have also demonstrated low neural damage and glial response due to their planar, macroporous morphology. Neural dust has not been widely used in CNS applications and provides minimal continual contact with the meningeal layers or subarachnoid space. Encapsulation of these devices may help to further improve their performance. Encapsulation of other form factors, such as the planar ECoG with silicon carbide has been demonstrated to improve biocompatibility and device longevity.<sup>[120]</sup>

Material selection plays a crucial role in the response of brain tissue toward implanted devices. Transition metals such as tungsten and silicon have relatively high rigidity and poor biocompatibility, which is primarily the result of corrosion.<sup>[161]</sup> To surmount this concern, metal electrodes are encapsulated with materials such as parylene-C, Teflon, and polyimide, which significantly reduce scarring, infection, and inflammation in neural tissue. As explored in Section 2, a further reduction in biological response has been achieved through the use of biomaterials which mimic the mechanical properties of the ECM.<sup>[58]</sup> These biomaterials include collagen, PEG hydrogels, and Matrigel. Less glial response was demonstrated with devices masked from the typical inflammatory pathway through the use of biomaterials described above.

Current and future neuroimplantable devices face a wide assortment of biological risk factors from the heterogeneous environment of the CNS. Despite these challenges, careful device design, materials choices, and implantation procedure can aid in the creation of hybrid neural interfaces that reduce adverse tissue response, decrease the frequency and severity of infections, and improve device lifetime.

## 5. Navigating the Regulatory Landscape of Neuroimplantable Devices

Regulatory agencies have established metrics to determine whether specific devices are reasonable for commercialization through parameters congruent to those discussed in Sections 2, 3, 4, including functionality, form factor, implantation procedure, and material selection. Among these agencies' regulatory processes, evaluation by the US FDA is considered a well-accepted standard. In this section, we i) discuss the US FDA regulatory environment and clinical approval process with regards to the unique challenges of neuroimplantable devices, ii) describe relevant screening for appropriate safety and efficacy, iii) relate clinical data to our earlier discussion of materials choices, and iv) summarize relevant failure points of market-approved devices.

The US FDA has set up three categories based on the level of control necessary to assure the safety and efficacy of neural interfaces. The classification system also considers both the intended use and evaluates the risk posed to the patient. A Class I device, having the lowest risk, requires only general controls such as registration, device listing, labeling, manufacturing standards, reporting, and sterility. A Class II device, having moderate risk, requires additional "special" controls in addition to the general controls, specific to the device design. Both classes can have exempt cases with limitations. A Class III device, having the greatest risk, generally requires PMA, which necessitates the collection of clinical data, satisfying minimal standards of safety and efficacy. In the case that the device is substantially equivalent to an FDA approved device and a PMA has not been called for, a 510(k) filing provides a pathway to market without the need for clinical data.<sup>[39]</sup>

In considering the optimal path to market for neurological device manufacturers, parameters such as functionality, form factor, implantation protocol, and material choices should be considered as part of the preclinical planning process. With the unique challenges presented through the advent of neuroimplantable devices, the FDA has typically approached its regulatory role with the classification of all transcranial tools in the high-risk Category III.<sup>[162]</sup> While the inherent risks posed by the rigorous and long approval in Category III devices can be a deterrent for technological development in the preclinical stage, a consideration of the risk factors and predicates considered by the FDA in the course of product evaluation can provide an ideal path to market in terms of reduced approval times and fewer regulatory hurdles.

### 5.1. FDA Regulatory Pathways in Relation to Probe Type, Form Factor, and Material Selection

As the device is implanted at greater depths into the brain, from extracranial to intracerebral, an increasing portion of the neural structure is exposed to disturbance or potential damage, which poses a higher risk to the user as described in Section 3.

Though de novo devices in Class II and III must often proceed through the FDA process by gathering clinical data, many devices (up to 90% in Class I) are exempt from this requirement due to the filing of a 510(k)-submission

demonstrating a substantial equivalence to an existing post-market FDA regulated device.<sup>[162]</sup> This determination of substantial equivalence is typically based on bench testing, the use of FDA consensus standards, and data from prior animal trials. One regulatory path used by de novo implantable devices has been the humanitarian device exemption (HDE), which is primarily targeted toward orphan diseases not affecting more than 4000 cases annually in the United States of America. The primary advantage of an HDE is that the "efficacy" requirement is suspended from the approval process. This process has been used previously to expedite the path to market for neuroimplantable devices.<sup>[163]</sup> This trend is well reflected in the classification of various devices targeted to the central nervous system. For example, the non-invasive EEG electrode poses few risks to users and is classified as Class I device.<sup>[162]</sup>

An ECoG electrode, which sits on top of the cortex, is classified as a Class II device.<sup>[164]</sup> Though it does not contain components which penetrate the cortex, it nonetheless requires a more invasive procedure than an EEG requires for implantation, namely an open craniotomy, thereby necessitating a higher classification.

Depth electrodes and shallow probes such as DBS or multielectrode arrays, are considered to be of the highest risk and, thus, are typically classified as Class III.<sup>[164]</sup> This is due to the invasive nature of the implantation, which requires an open craniotomy, and concerns about the long-term stability of deeply penetrating electrodes.

As described in Section 2, the FDA has approved a number of neural interfacing devices with predicate materials such as tungsten,<sup>[14]</sup> stainless steel,<sup>[14]</sup> silicon,<sup>[165]</sup> polyimide,<sup>[14]</sup> and parylene-C,<sup>[15]</sup> amongst others. Given that biocompatibility requirements have been demonstrated for all predicates, a path for expedited approval can be achieved through incorporation of these materials into new probe designs. Furthermore, fabrication protocols which encapsulate the final device in an FDA-approved flexible substrate reduce local inflammation and, subsequently, may not require additional biocompatibility screening.

For example, in 2011, the FDA approved a new version of the Blackrock microsystems Neuroport brain computing interface.<sup>[13,164]</sup> This was an amendment on a predicate Neuroport system, which had prior approval. Though the system added a number of new features including support for ECoG, electrooculography (EOG), and EEG, the lack of any substantial changes to the probe layout and the coating materials did not necessitate additional biocompatibility or safety testing in model animals or in humans. Additionally, this allowed the system achieve approval for longer implantation periods, once again without the need for additional testing. In this case, the new device was approved for an implantation lifetime of 30 d.<sup>[13]</sup> A consideration of predicate materials and designs can be a valuable consideration in accelerating the path to market for a commercial system.

### 5.2. Relevant Clinical Results Related to Mechanical and Biological Risk Factors

Despite the risks associated with deep brain implants, direct hazards—such as infection, continual inflammation, and

hemorrhaging—occur relatively infrequently, as described in Section 4. Clinical data has consistently concluded that the majority of failure points in neuroimplantable devices are fundamentally mechanical in nature. Third-party evaluations by Barrese et al. determined that the primary failure points of silicon-based intracortical arrays in nonhuman primates occurred within the first year of implantation.<sup>[139]</sup> Specifically, 56% of the devices failed within the first 12 months and 48% of the failures could be attributed to mechanical malfunctions. Additionally, 83% of the mechanical failures were primarily due to issues with connectors, rather than with the implants themselves. Biological failures accounted for 24% of the observable terminations and primarily resulted from a meningeal reaction that abstracted the brain tissue from the array, reducing the fidelity of recording, but without presenting an immediate health risk to the end user.

In a retrospective analysis of data from a single medical center on DBS on PD patients, conducted by Shanghai Jiao Tong University, 41 cases of deaths were reported during the 16 years of follow-ups after implantation.<sup>[166]</sup> Among these lethal cases, only 2 were due to intracranial hemorrhage, making up 0.4% of the total. Additionally, 22 (4.6%) cases of nonlethal, biological complications related to the probe material were reported, of which 11 (2%) were cases of immune rejection and 9 (1.8%) were cases of infection. Though neural probes present considerable risk due to the invasiveness of implantation, cases of death from hemorrhage and infection are relatively uncommon.

In a study conducted by Mischer Neuroscience Institute involving 728 patients with DBS electrode implantation, the occurrence of hemorrhaging was 5%, among which the majority was intraventricular (3.4%), and the remaining 1.6% being intracerebral.<sup>[167]</sup> Additionally, the occurrence of ischemic infarction, a sudden loss of circulation to a portion of the brain, was 0.4%. By comparison, 1.7% of the failures resulted from wound infections, 1.7% from probe malposition/migration, and 1.4% from component fracture. 0.5% of cases resulted from component malfunction and 2.6% from loss of efficacy, necessitating removal, were reported, making a total 7.9% of hardware-related complications. While certain cases of acute biological failures were present, the primary complication was mechanical, due to form factor and probe material.

In the total product life cycle of FDA-approved intracerebral stimulators for pain relief, all the reported cases (*n* of 6) are either electrical (impedance) or mechanical (migratory) in nature. Similar trends can also be found for implanted subcortical electrical stimulators. Of the 1012 reported device problems, more than 70% are identified as hardware-related (e.g., impedance too high or low, battery malfunction or connection issues).<sup>[168]</sup>

For example, in the FDA summary of safety and effectiveness for the Brio Neurostimulation System, a Class III implanted electrical stimulator for Parkinsonian tremors, 5 (5%) cases of infection and 4 (4%) cases of intracranial hemorrhage were reported out of the total of 101 stimulations.<sup>[168]</sup> Although biocompatibility screening is highly advantageous for prevention of acute trauma, mechanical failures constitute the primary failure point of medically approved neuroimplantable instruments.

Advances in probe design and fabrication may help to address the mechanical failures that are predominant amongst FDA approved devices. For example, novel flexible thin film

materials such as polyimide and parylene used in the fabrication of shanks may help to alleviate fracturing and degradation of the probe systems, decreasing power leakage by up to 80%<sup>[36]</sup> and reducing neural damage fivefold.<sup>[131]</sup> Furthermore, the inherent longitudinal degradation of shanks has been shown to be partially alleviated by creating a hybrid neural interface through the use of mechanically matched hydrogel coatings<sup>[49]</sup> or through the use of substrate materials such as collagen that naturally exist in the body.<sup>[58]</sup> Novel developments in probe form and materials are poised to reduce mechanical and biological risks, thereby expediting medical clearance.

### 5.3. Primary Failure Points of Postmarket Approval Devices

Though devices routinely undergo *in vitro* testing as well as animal and human preclinical and clinical trials, device recalls are not uncommon in the postapproval environment. Based on the potential risk level, the FDA has also set up a three-class hierarchy for device recall. Class I recalls are considered the highest urgency, while Class II and Class III recalls have appropriately diminishing risk profiles in terms of severity. Reasons for recall of neuroimplantable devices include mechanical failure of the mounting components,<sup>[169]</sup> abrasion to cortical surfaces due to fracturing of electrodes,<sup>[170]</sup> malfunctions to the recording equipment,<sup>[171]</sup> and software failures during implantation resulting in suboptimal placement of electrodes.<sup>[172]</sup> Notably, few of documented recalls are caused by unacceptable rates of infection or hemorrhaging of brain vasculature.

For instance, a Class I recall was filed in 2013 for the Activa Dystonia Therapy Kit, a Medtronic, Inc., product, due to potential DBS lead damage caused by setscrew connect design.<sup>[173]</sup> Notably, this recall due to mechanical failure is the only recorded case on the FDA database for not only this specific product but also for implanted subcortical electrical stimulators in general. A Class II recall of the Integra Life Sciences Ojemann Cortical Stimulator, also filed in 2013, which concerns potential nonintended voltage injury, was also caused by an issue related to device design rather than biocompatibility.<sup>[174]</sup>

Additionally, most FDA device recalls are concentrated in devices with predicates that did not necessitate additional clinical data during approval. Out of devices recalled between 2005 and 2009, 71% had been approved through a 510(k) filing by demonstrating substantial equivalence to an existing device.<sup>[175]</sup> In many cases, 510(k) filings provide an effective route to market for devices with provable similarity to FDA predicates, creating a faster turnaround time for life-altering therapies. Taking mechanical failure points into consideration before market approval, however, may reduce the risks of recall or operational hazards to end users. Additionally, predicate-based acceleration of *de novo* devices might miss important details, and precautions should be taken to prevent downstream risk of recalls.

### 5.4. Considerations for Materials Evaluation in the Regulatory Process

Notably for industry engineers, there currently exists no single set of FDA biocompatibility standards for long-term implanted

devices; however, several existing standards documents overlap with medical device testing guidelines and may be considered in the design process.<sup>[39]</sup>

The FDA conducts unique in-agency research for determination of clinical viability of materials and establishment of testing protocols for eventual use in the clinical setting. Specifically, through the office of science and engineering laboratories at the center of devices and radiological health (CDRH OSEL) research program, the FDA has been conducting studies for the durability of cortical implants under accelerated aging,<sup>[176]</sup> establishing systems for evaluating traumatic brain injury postimplantation,<sup>[177]</sup> and studying vascular dynamics following electrode implantation.<sup>[178]</sup> Additionally, the FDA has partnered with the DARPA reliable neural interface technology (RE-NET) program to help determine the long-term safety and efficacy of neuroimplantable devices.<sup>[39]</sup> The intended purpose of this collaboration between OSEL and RE-NET is the creation of a common test platform for independent testing of medical devices.

Concerning the use of materials, the FDA recognizes certain standards developed by third parties such as the international organization for testing and materials (ASTM). ASTM's international materials database provides information on how different materials have been utilized in clinically approved medical devices.<sup>[39]</sup> Materials which have been shown to be biocompatible in predicate devices can expedite approval of de novo device constructs.<sup>[39]</sup>

The factors considered relevant to biocompatibility assessment of materials and devices are cytotoxicity, sensitization, hemocompatibility, pyrogenicity, implantation length, genotoxicity, carcinogenicity, and developmental toxicity.<sup>[38]</sup> The FDA recommends a chemical assessment of the material prior to clinical testing. A full description of the FDA approval system as well as general biocompatibility guidelines for various probe types can be found in **Figure 9**. Representative materials used in devices that are currently approved by the FDA, as well as their organization by class, is shown in **Figure 10**. A number of clinical publications have determined the overall biocompatibility of known materials such as silicon,<sup>[179]</sup> tungsten,<sup>[180]</sup> iridium oxide,<sup>[181]</sup> parylene-C,<sup>[182]</sup> and PEDOT.<sup>[183]</sup>

### 5.5. Regulatory Considerations for Incorporating Novel Materials in Neuroimplantable Devices

Current advances in materials engineering and implantation strategies have led to the creation of conformable, hybrid devices that have the ability to efficiently record and stimulate neural tissue, deliver drugs transcranially, and resist biological degradation and scarring.<sup>[1]</sup> Through developments of both transcranial and peripheral sensory recording, far-reaching applications—such as full motor restoration in artificial human limbs and drug delivery which bypasses the blood–brain barrier—are entering the realm of possibility.<sup>[199]</sup>

Novel materials used for the fabrication of neural probes and coatings are subject to FDA regulations in higher classes due to i) the lack of predicate devices and ii) the unique challenges presented by these new material classes.<sup>[39]</sup> This has led to new testing and evaluation criteria for the FDA prior to approval for market use. For example, in situ polymerization of substrates used in

neural probes require additional screening to control for cytotoxicity and cross-reactivity.<sup>[38]</sup> ECM-based thin films, such as collagen scaffolds, have the potential to improve overall biocompatibility and mechanical properties but due to a lack of a predicate, however, in vivo studies and cytotoxicity and oncogenicity standards must be met for novel devices.<sup>[22]</sup> Although general guidance documents exist, early communication with CDRH can help to provide more targeted insurance of meeting compliance standards. Innovators can utilize the medical fellowship device program (MDFP) and the critical path initiative (CPI) for early communication with CDRH.<sup>[200]</sup> The current regulatory environment provides many hurdles for premarket technologies, but paths for expedited approval exist and should be considered early in the research process, in tandem with the design phase.<sup>[39]</sup> As described in the above sections, a careful consideration the materials choices, form factor, functionality, and implantation or delivery method is crucial, as these points are integral to regulatory pipeline.

For emerging companies in the field of neuroimplantable devices, the paths to market will involve both engineering and regulatory hurdles. Some strategies for navigating these hurdles include i) seeking predicates within approved devices through a 510(k) pathway and ii) pursuing the FDA innovation pathway, which is designed to accelerate the submission process through an active engagement with the FDA review team and senior science staff.<sup>[39]</sup> For intrinsically high-risk Class III devices, the FDA encourages an iterative improvement process, with an eventual target of approval and clearance to market. More than 60% of original PMAs received major deficiency letters on initial FDA reviews for the past five years (this number was 91% for year 2016), and more than 80% received final approvals (89% for year 2016; 84% for year 2018).<sup>[201]</sup> Though certain standards for biocompatibility and predicates exist, the approval process is highly specific to each device, and, therefore, is judged on a case-by-case basis. As described above, early communication with CDRH, appropriate selection of a clinical path, and an iterative development pipeline should be pursued for an overall quicker path to market.

Despite their interest in novel neuroimplantable devices, the FDA does not currently have a regulatory pathway suitable for nonclinical implantable technologies, whether for neurological applications or otherwise. As a result, navigating nonclinical paths to approval presents even greater challenges than the standard clinical pipeline. Some in the medical research community have suggested addressing these challenges through the addition of new regulatory classes to the current FDA environment. These new regulatory categories would be tasked with the regulation of de novo devices for cognitive enhancement and other nonclinical applications.<sup>[202]</sup> It is still unclear whether a current path forward for a nonclinical tool exists within the regulatory environment of the US FDA.

### 5.6. Global Regulation of Neuroimplantable Devices

Certain device manufacturers who have been interested in pursuit of targeting a global device market have inevitably come into contact with different regulatory frameworks from Europe to Asia-Pacific. Within the European union (EU), regulation of medical devices is handled through the EU medical device

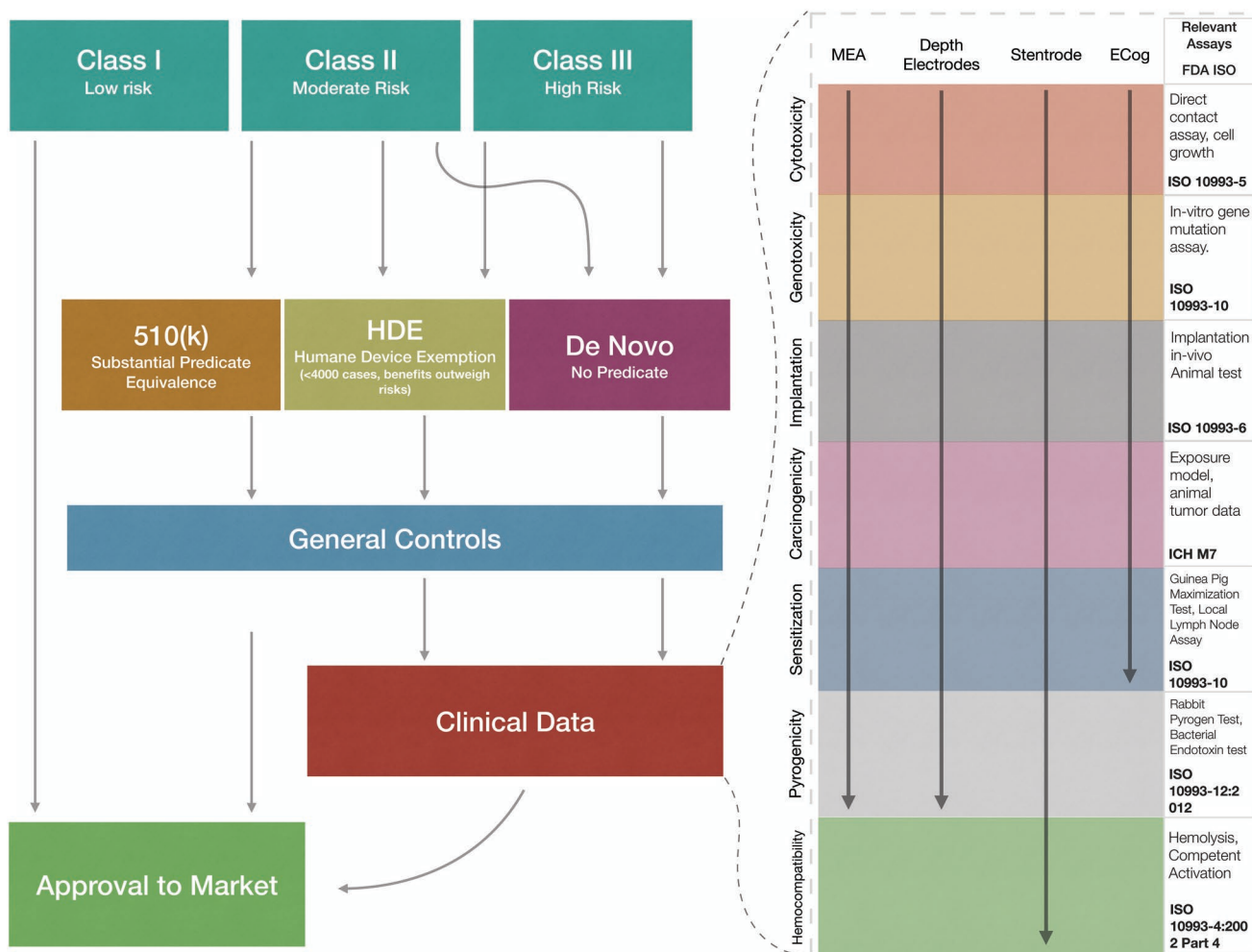


**Figure 9.** An overview of the common regulatory pathways for neuroimplantable devices. New medical device submissions are assigned a class based on their level of risk, their target diseases, and the existence of device predicates. Devices with predicates from Classes I and II may utilize the 510(k) process of submission, which permits circumvention of the need for clinical data, but still requires standard general controls (including registration, device listing, labeling, manufacturing standards, reporting, and sterility). Devices that target diseases with an incidence rate below 4000 cases may utilize the humane device exemption (HDE), which requires both controls and collection of clinical data but is exempt from the efficacy requirements for de novo devices. Higher risk devices without predicates or an HDE must pursue a de novo pathway, which requires adherence to general controls and submission of clinical data demonstrating an appropriate standard of safety and efficacy. In the course of clinical data collection for novel materials without predicates, the FDA recognizes biocompatibility standards,<sup>[38]</sup> including tests for cytotoxicity, sensitization, implantation, genotoxicity, carcinogenicity, pyrogenicity, and hemocompatibility. However, relevant assays for the establishment of these standards is not uniform for all probe types. We demonstrate potential biocompatibility tests for various devices. For example, while MEAs and depth electrodes require screening for pyrogenicity due to their contact with cerebrospinal fluid in the course of implantation, epidural ECog devices do not. Stentrodes have continual contact with blood and cerebrospinal fluid and, therefore, would potentially require hemocompatibility screening.

regulation (MDR), which has been in effect since 2017.<sup>[203]</sup> Similar to US regulations by the FDA, the MDR is built around a three class system with Class III medical devices posing the greatest risk to consumers and Class I devices being considered the safest.<sup>[204]</sup> Most notably, the European approval process operates through a network of decentralized agencies among the EU member states.<sup>[204]</sup> Though many of the necessary premarket tests for safety and efficacy are similar between the European market and the United States, there are differences in specific timelines and necessary data for renewal of certificates and initial approval. In addition, there are specific standards defined by each member state. Approval under either

the European regulatory framework or the FDA does not necessarily imply an expedited path in other nation states. Despite this, efforts by the U.S. Congress are underway to facilitate approval of devices which have already gained approval in Europe. Further complications to this process involve variation in the definition of what constitutes a Class I, II, or III device.<sup>[205]</sup> Though general guidelines are similar, there is often disagreement on the global risk of individual devices.

In Japan, regulation of medical devices is the responsibility of the pharmaceuticals and medical devices agency (PMDA). Unlike in the EU and US, the Japanese regulatory system operates on a class system ranging from Class I to Class IV,

	Class I		Class II		Class III	
	Electrode	Encapsulation	Electrode	Encapsulation	Electrode	Encapsulation
Common Materials in Approved Devices						
Representative commercial products	Company with approved product		Company with approved product		Company with approved product	
	Name of product		Name of product		Name of product	
	World Precision Instruments	Electroencephalograph electrode	Micromed	Cortical Electrode	Neuropace	Implanted Brain Stimulator For Epilepsy
	Integra Neurosciences	Ventricular cannula	Ad-Tech	Cable, Electrode	ReShape Lifesciences, Inc.	Neuromodulator For Obesity
			Dixi Medical	Electrode, Depth	Medtronic	Stimulator, Electrical, Implanted, For Parkinsonian Tremor
		Nihon Kohden Co.	Amplitude-Integrated Electroencephalograph	Abbott Medical	Stimulator, Electrical, Implanted, For Parkinsonian Tremor	

**Figure 10.** A representative table demonstrating FDA-approved devices targeting the central nervous system, organized by FDA class, by the company and name of device (as specified by the FDA), and by common substrate and electrode materials found within approved devices in each class. Representative Class I devices include the World Precision Instruments electroencephalograph (EEG) electrode<sup>[184,185]</sup> and the Integra Neurosciences ventricular cannula.<sup>[186]</sup> Representative Class II devices include the Micromed cortical electrode,<sup>[187,188]</sup> the Ad-Tech cortical electrode (cable, electrode),<sup>[189]</sup> the Dixi Medical depth electrode,<sup>[190,191]</sup> and the Nihon Kohden Corporation Amplitude-Integrated EEG.<sup>[192,193]</sup> Representative Class III devices include the Neuropace implanted brain stimulator for epilepsy,<sup>[17,194]</sup> the ReShape Lifesciences, Inc., neuromodulator for obesity,<sup>[195,196]</sup> the Medtronic implanted electrical stimulator for Parkinsonian tremors,<sup>[32,197]</sup> and the Abbott Medical implanted electrical stimulator for Parkinsonian tremors.<sup>[197,198]</sup> Abbreviations: Ag: silver, Au: gold, PDMS: polydimethylsiloxane, Sil-Rubber: silicone rubber, Pt: platinum, Ir: iridium, Si: silicon, Ti: titanium, PUR: polyurethane. Note that this figure does not imply that use of a certain material will result in assignment into the stated class, and class designations are based on predicates and are provided for reference only.

with higher classes being associated with higher risk to the end user.<sup>[206]</sup> Though the Japanese process of approval is also distinct and separate from that of the FDA, in recent years, attempts have been made by the two agencies to harmonize standards for approval to expedite medical device innovation.<sup>[207]</sup>

Despite the challenges involved, a steadily growing number of devices for a wide array of clinical applications have made their way to market.<sup>[201]</sup> Individuals, academic institutions, and for-profit commercial entities must engage with both regulatory oversight agencies and the public at an early stage of research to best determine the paths to commercial viability.

## 6. Conclusion

This review summarizes the progress and ongoing challenges in developing neuroimplantable devices—from the perspectives of materials engineering, device implantation, associated biological risk factors, and the FDA regulatory landscape. Development and commercialization of novel devices is a daunting task for medical innovators encompassing mechanical, biological, and regulatory

challenges. Addressing these considerations and utilizing risk management strategies is possible through the integration of conformable features, flexible geometries, and hybrid materials. Additionally, in the device design phase, early communication with FDA regulators can expedite the path to market of de novo technologies. These next-generation devices will enable researchers and physicians to better interrogate and perturb neural circuitry, shedding light on our understanding of neurodegenerative diseases and opening paths to robust therapeutic cures. Collectively, the improvements in neuroimplantable devices with advancements in biocompatible materials, device form factors, and implantation techniques will afford us new opportunities to explore the brain and provide treatment strategies for various neuronal disorders.

## Acknowledgements

N.O. and F.T. contributed equally to this work. The authors thank David Sadat, Tao Sun, and Zijun Wei for assisting with the manuscript preparation. All authors contributed to the manuscript writing. The research was supported by MIT Media Lab.

## Conflict of Interest

The authors declare no conflict of interest.

## Keywords

biocompatible materials, brain–computer interfaces, conformable hybrid devices, FDA regulatory processes, neuroimplantable devices

Received: March 6, 2019

Revised: April 12, 2019

Published online:

- [1] J. Rivnay, H. Wang, L. Fenno, K. Deisseroth, G. G. Malliaras, *Sci. Adv.* **2017**, 3, e1601649.
- [2] W. Penfield, *Arch. Neurol. Psychiatry* **1936**, 36, 449.
- [3] K. M. Szostak, L. Grand, T. G. Constantinou, *Front. Neurosci.* **2017**, 11, 665.
- [4] J. C. Leiter, M. M. Chernov, D. W. Roberts, *US20100312305A1*, **2010**.
- [5] E. S. Boyden, *F1000 Biol. Rep.* **2011**, 3, 11.
- [6] C. Dagdeviren, K. B. Ramadi, P. Joe, K. Spencer, H. N. Schwerdt, H. Shimazu, S. Delcasso, K.-I. Amemori, C. Nunez-Lopez, A. M. Graybiel, M. J. Cima, R. Langer, *Sci. Transl. Med.* **2018**, 10, eaan2742.
- [7] F. V. Tenore, R. J. Vogelstein, *Johns Hopkins APL Tech. Dig.* **2011**, 30, 230.
- [8] A. K. Engel, C. K. E. Moll, I. Fried, G. A. Ojemann, *Nat. Rev. Neurosci.* **2005**, 6, 35.
- [9] E. D. Adrian, *BMJ* **1954**, 1, 287.
- [10] J. Krüger, F. Caruana, R. D. Volta, G. Rizzolatti, *Front. Neuroeng.* **2010**, 3, 6.
- [11] K. Badstübner, T. Kröger, E. Mix, U. Gimsa, R. Benecke, J. Gimsa, *Biomedical Engineering Systems and Technologies*, Springer, Berlin **2013**, pp. 287–297.
- [12] J. D. Simeral, S.-P. Kim, M. J. Black, J. P. Donoghue, L. R. Hochberg, *J. Neural Eng.* **2011**, 8, 025027.
- [13] United States Food and Drug Administration, *510(k) Summary NeuroPort™ Electrode (SIROF) K110010*, **2011**.
- [14] United States Food and Drug Administration, *510(k) Summary AccuPoint™ Electrode K162459*, **2017**.
- [15] United States Food and Drug Administration, *510(k) Summary RTI Surgical, Inc., Nerve Monitoring Cable System K142438*, **2015**.
- [16] United States Food and Drug Administration, *510(k) Summary Longevity PMMA Static Cranial Implant K170410*, **2018**.
- [17] United States Food and Drug Administration, *Pre-Market Approval (PMA) Summary, Neuropace RNS System, ID P100026*, **2013**.
- [18] R. A. Normann, E. Fernandez, *J. Neural Eng.* **2016**, 13, 061003.
- [19] L. A. French, J. L. Story, J. H. Galicich, E. A. Schultz, *Stereotact. Funct. Neurosurg.* **1962**, 22, 265.
- [20] L. F. Haas, *J. Neurol. Neurosurg. Psychiatry* **2003**, 74, 9.
- [21] O. Foerster, H. Altenburger, *Dtsch. Z. Nervenheilkd.* **1935**, 135, 277.
- [22] F. Panov, E. Levin, C. de Hemptinne, N. C. Swann, S. Qasim, S. Miocinovic, J. L. Ostrem, P. A. Starr, *J. Neurosurg.* **2017**, 126, 122.
- [23] T. D. Y. Kozai, *Micromachines* **2018**, 9, 445.
- [24] K. Wise, J. Angell, *Solid-State Circuits Conf. Digest of Technical Papers*, IEEE International, Philadelphia, PA **1971**, pp. 100–101.
- [25] K. E. Jones, P. K. Campbell, R. A. Normann, *Ann. Biomed. Eng.* **1992**, 20, 423.
- [26] Z. Zhao, E. Kim, H. Luo, J. Zhang, Y. Xu, *J. Micromech. Microeng.* **2018**, 28, 015012.
- [27] P. Fattahi, G. Yang, G. Kim, M. R. Abidian, *Adv. Mater.* **2014**, 26, 1846.
- [28] D. Seo, R. M. Neely, K. Shen, U. Singhal, E. Alon, J. M. Rabaey, J. M. Carmena, M. M. Maharbiz, *Neuron* **2016**, 91, 529.
- [29] J. Gardner, *Soc. Stud. Sci.* **2013**, 43, 707.
- [30] F. Munding, *Stereotact. Funct. Neurosurg.* **1965**, 26, 222.
- [31] P. L. Gildenberg, *Fifty Years of Neurosurgery*, Lippincott Williams & Wilkins, New York, NY **2000**, p. 295.
- [32] United States Food and Drug Administration, *Pre-Market Approval (PMA) Summary, Medtronic Activa Parkinson's Control System, ID P960009/S007*, **2002**.
- [33] United States Food and Drug Administration, *Pre-Market Approval (PMA) Summary, Medtronic DBS Therapy for Epilepsy, ID P960009/S219*, **2018**.
- [34] E. S. Boyden, F. Zhang, E. Bamberg, G. Nagel, K. Deisseroth, *Nat. Neurosci.* **2005**, 8, 1263.
- [35] K. B. Ramadi, C. Dagdeviren, K. C. Spencer, P. Joe, M. Cotler, E. Rousseau, C. Nunez-Lopez, A. M. Graybiel, R. Langer, M. J. Cima, *Proc. Natl. Acad. Sci. USA* **2018**, 115, 7254.
- [36] J. H. Kim, G. H. Lee, S. Kim, H. W. Chung, J. H. Lee, S. M. Lee, C. Y. Kang, S.-H. Lee, *Biosens. Bioelectron.* **2018**, 117, 436.
- [37] L. Anderson, P. Antkowiak, A. Asefa, A. Ballard, T. Bansal, A. Bello, B. Berne, K. Bowsher, B. Blumenkopf, I. Broverman, M. Bydon, K. Chao, P. Como, K. Cork, A. Costello, K. De Laurentis, A. DeMarco, H. Dean, J. Doucet, B. Dworak, L. Epperson, E. Franca, N. Ghassemian, C. Ghosh, A. Govindarajan, J. Gupta, S. Gutowski, R. Herrmann, M. Hoffmann, W. Heetderks, S. Hsu, D. Kaufman, E. Keegan, G. Kittlesen, K. Khoo, H. Lee, L. Lo, I. Marcus, T. Marjenin, B. Mathews, S. Misra, V. Pinto, V. Ramos, S. Raben, A. Russell, D. Saha, J. Seog, C. Shenouda, M. Smith, X. Tang, K. Wachrathit, J. Waterhouse, D. Williams, X. Zheng, C. Peña, *Neuron* **2016**, 92, 943.
- [38] International Organization for Standardization, *Biological Evaluation of Medical Devices-Part 1: Evaluation and Testing within a Risk Management Process*, **2016**.
- [39] C. Welle, V. Krauthamer, *IEEE Pulse* **2012**, 3, 37.
- [40] S. Budday, R. Nay, R. de Rooij, P. Steinmann, T. Wyrobek, T. C. Ovaert, E. Kuhl, *J. Mech. Behav. Biomed. Mater.* **2015**, 46, 318.
- [41] G. T. Fallenstein, V. D. Hulse, J. W. Melvin, *J. Biomech.* **1969**, 2, 217.
- [42] K. Miller, K. Chinzei, G. Orssengo, P. Bednarsz, *J. Biomech.* **2000**, 33, 1369.
- [43] P. C. Georges, W. J. Miller, D. F. Meaney, E. S. Sawyer, P. A. Janmey, *Biophys. J.* **2006**, 90, 3012.
- [44] Y.-B. Lu, K. Franze, G. Seifert, C. Steinhäuser, F. Kirchoff, H. Wolburg, J. Guck, P. Janmey, E.-Q. Wei, J. Käs, A. Reichenbach, *Proc. Natl. Acad. Sci. USA* **2006**, 103, 17759.
- [45] Z. J. Du, C. L. Kolarcik, T. D. Y. Kozai, S. D. Luebben, S. A. Sapp, X. S. Zheng, J. A. Nabity, X. T. Cui, *Acta Biomater.* **2017**, 53, 46.
- [46] R. Chen, A. Canales, P. Anikeeva, *Nat. Rev. Mater.* **2017**, 2, 16093.
- [47] K. Scholten, E. Meng, *Lab Chip* **2015**, 15, 4256.
- [48] S. M. Won, E. Song, J. Zhao, J. Li, J. Rivnay, J. A. Rogers, *Adv. Mater.* **2018**, 30, 1800534.
- [49] K. C. Spencer, J. C. Sy, K. B. Ramadi, A. M. Graybiel, R. Langer, M. J. Cima, *Sci. Rep.* **2017**, 7, 1952.
- [50] C. D. Lee, S. A. Hara, L. Yu, J. T. W. Kuo, B. J. Kim, T. Hoang, V. Pikov, E. Meng, *J. Biomed. Mater. Res., Part B* **2016**, 104, 357.
- [51] J. Pas, A. L. Rutz, P. P. Quilichini, A. Slézia, A. Ghestem, A. Kaszas, M. J. Donahue, V. F. Curto, R. P. O'Connor, C. Bernard, A. Williamson, G. G. Malliaras, *J. Neural Eng.* **2018**, 15, 065001.
- [52] F. Wu, L. W. Tien, F. Chen, J. D. Berke, D. L. Kaplan, E. Yoon, *J. Microelectromech. Syst.* **2015**, 24, 62.
- [53] F. Vitale, W. Shen, N. Driscoll, J. C. Burrell, A. G. Richardson, O. Adewole, B. Murphy, A. Ananthkrishnan, H. Oh, T. Wang, T. H. Lucas, D. K. Cullen, M. G. Allen, B. Litt, *PLoS One* **2018**, 13, e0206137.

- [54] S.-J. Kim, S. C. Manyam, D. J. Warren, R. A. Normann, *Ann. Biomed. Eng.* **2006**, *34*, 300.
- [55] United States Food and Drug Administration, 510(k) Summary, *Ad-Tech Subdural Electrode*, ID K970587, **1997**.
- [56] K. Tybrandt, D. Khodagholy, B. Dielacher, F. Stauffer, A. F. Renz, G. Buzsáki, J. Vörös, *Adv. Mater.* **2018**, *30*, 1706520.
- [57] K. J. Yu, D. Kuzum, S.-W. Hwang, B. H. Kim, H. Juul, N. H. Kim, S. M. Won, K. Chiang, M. Trumpis, A. G. Richardson, H. Cheng, H. Fang, M. Thomson, H. Bink, D. Talos, K. J. Seo, H. N. Lee, S.-K. Kang, J.-H. Kim, J. Y. Lee, Y. Huang, F. E. Jensen, M. A. Dichter, K. H. Lucas, J. Viventi, B. Litt, J. A. Rogers, *Nat. Mater.* **2016**, *15*, 782.
- [58] W. Shen, L. Karumbaiah, X. Liu, T. Saxena, S. Chen, R. Patkar, R. V. Bellamkonda, M. G. Allen, *Microsyst. Nanoeng.* **2015**, *1*, 15010.
- [59] T. J. Oxley, N. L. Opie, S. E. John, G. S. Rind, S. M. Ronayne, T. L. Wheeler, J. W. Judy, A. J. McDonald, A. Dornom, T. J. H. Lovell, C. Steward, D. J. Garrett, B. A. Moffat, E. H. Lui, N. Yassi, B. C. V. Campbell, Y. T. Wong, K. E. Fox, E. S. Nurse, I. E. Bennett, S. H. Bauquier, K. A. Liyanage, N. R. van der Nagel, P. Perucca, A. Ahnood, K. P. Gill, B. Yan, L. Churilov, C. R. French, P. M. Desmond, M. K. Horne, L. Kiers, S. Prawer, S. M. Davis, A. N. Burkitt, P. J. Mitchell, D. B. Grayden, C. N. May, T. J. O'Brien, *Nat. Biotechnol.* **2016**, *34*, 320.
- [60] J. J. Jun, N. A. Steinmetz, J. H. Siegle, D. J. Denman, M. Bauza, B. Barbarits, A. K. Lee, C. A. Anastassiou, A. Andrei, Ç. Aydın, M. Barbic, T. J. Blanche, V. Bonin, J. Couto, B. Dutta, S. L. Gratiy, D. A. Gutnisky, M. Häusser, B. Karsh, P. Ledochowitsch, C. M. Lopez, C. Mitelut, S. Musa, M. Okun, M. Pachitariu, J. Putzeys, P. D. Rich, C. Rossant, W.-L. Sun, K. Svoboda, M. Carandini, K. D. Harris, C. Koch, J. O'Keefe, T. D. Harris, *Nature* **2017**, *551*, 232.
- [61] J. Liu, T.-M. Fu, Z. Cheng, G. Hong, T. Zhou, L. Jin, M. Duvvuri, Z. Jiang, P. Kruskal, C. Xie, Z. Suo, Y. Fang, C. M. Lieber, *Nat. Nanotechnol.* **2015**, *10*, 629.
- [62] G. Shin, A. M. Gomez, R. Al-Hasani, Y. R. Jeong, J. Kim, Z. Xie, A. Banks, S. M. Lee, S. Y. Han, C. J. Yoo, J.-L. Lee, S. H. Lee, J. Kurniawan, J. Tureb, Z. Guo, J. Yoon, S.-I. Park, S. Y. Bang, Y. Nam, M. C. Walicki, V. K. Samineni, A. D. Mickle, K. Lee, S. Y. Heo, J. G. McCall, T. Pan, L. Wang, X. Feng, T.-I. Kim, J. K. Kim, Y. Li, Y. Huang, R. W. Gereau 4th, J. S. Ha, M. R. Bruchas, J. A. Rogers, *Neuron* **2017**, *93*, 509.
- [63] A. Canales, X. Jia, U. P. Froriep, R. A. Koppes, C. M. Tringides, J. Selvidge, C. Lu, C. Hou, L. Wei, Y. Fink, P. Anikeeva, *Nat. Biotechnol.* **2015**, *33*, 277.
- [64] U.S. National Library of Medicine, *ECOG Direct Brain Interface for Individuals With Upper Limb Paralysis—Clinical Trial NCT01393444*, **2011**.
- [65] W. Wang, A. D. Degenhart, J. L. Collinger, R. Vinjamuri, G. P. Sudre, P. D. Adelson, D. L. Holder, E. C. Leuthardt, D. W. Moran, M. L. Boninger, A. B. Schwartz, D. J. Crammond, E. C. Tyler-Kabara, D. J. Weber, *Conf. Proc. IEEE Eng. Med. Biol. Soc.* **2009**, *2009*, 586.
- [66] D.-H. Kim, J. Viventi, J. J. Amsden, J. Xiao, L. Vigeland, Y.-S. Kim, J. A. Blanco, B. Panilaitis, E. S. Frechette, D. Contreras, D. L. Kaplan, F. G. Omenetto, Y. Huang, K.-C. Hwang, M. R. Zakin, B. Litt, J. A. Rogers, *Nat. Mater.* **2010**, *9*, 511.
- [67] R. A. Green, P. B. Matteucci, R. T. Hassarati, B. Giraud, C. W. D. Dodds, S. Chen, P. J. Byrnes-Preston, G. J. Suaning, L. A. Poole-Warren, N. H. Lovell, *J. Neural Eng.* **2013**, *10*, 016009.
- [68] H. Jasper, W. Penfield, *Arch. Psychiatr. Nervenkrankh.* **1949**, *183*, 163.
- [69] F. Rosenow, H. Lüders, *Brain* **2001**, *124*, 1683.
- [70] E. Asano, C. Juhász, A. Shah, S. Sood, H. T. Chugani, *Brain* **2009**, *132*, 1038.
- [71] N. Sinha, J. Dauwels, M. Kaiser, S. S. Cash, M. Brandon Westover, Y. Wang, P. N. Taylor, *Brain* **2017**, *140*, 319.
- [72] C. Henle, M. Schuettler, J. Rickert, T. Stieglitz, in *Towards Practical Brain–Computer Interfaces: Bridging the Gap from Research to Real-World Applications* (Eds: B. Z. Allison, S. Dunne, R. Leeb, J. D. R. Millán, A. Nijholt), Springer, Berlin **2013**, pp. 85–103.
- [73] J. A. Rogers, T. Someya, Y. Huang, *Science* **2010**, *327*, 1603.
- [74] M. A. Meitl, Z.-T. Zhu, V. Kumar, K. J. Lee, X. Feng, Y. Y. Huang, I. Adesida, R. G. Nuzzo, J. A. Rogers, *Nat. Mater.* **2006**, *5*, 33.
- [75] T.-H. Kim, A. Carlson, J.-H. Ahn, S. M. Won, S. Wang, Y. Huang, J. A. Rogers, *Appl. Phys. Lett.* **2009**, *94*, 113502.
- [76] A. Carlson, A. M. Bowen, Y. Huang, R. G. Nuzzo, J. A. Rogers, *Adv. Mater.* **2012**, *24*, 5284.
- [77] C. Linghu, S. Zhang, C. Wang, J. Song, *npj Flexible Electron.* **2018**, *2*, 26.
- [78] Y. K. Lee, K. J. Yu, E. Song, A. Barati Farimani, F. Vitale, Z. Xie, Y. Yoon, Y. Kim, A. Richardson, H. Luan, Y. Wu, X. Xie, T. H. Lucas, K. Crawford, Y. Mei, X. Feng, Y. Huang, B. Litt, N. R. Aluru, L. Yin, J. A. Rogers, *ACS Nano* **2017**, *11*, 12562.
- [79] S. Watanabe, H. Takahashi, K. Torimitsu, *Jpn. J. Appl. Phys.* **2017**, *56*, 037001.
- [80] M. P. Ward, P. Rajdev, C. Ellison, P. P. Irazoqui, *Brain Res.* **2009**, *1282*, 183.
- [81] K. D. Wise, J. B. Angell, A. Starr, *IEEE Trans. Biomed. Eng.* **1970**, *17*, 238.
- [82] Z. Fekete, *Sens. Actuators, B* **2015**, *215*, 300.
- [83] R. Bhandari, S. Negi, F. Solzbacher, *Biomed. Microdevices* **2010**, *12*, 797.
- [84] A. Goryu, R. Numano, A. Ikeda, M. Ishida, T. Kawano, *Nanotechnology* **2012**, *23*, 415301.
- [85] W.-T. Tseng, C.-T. Yen, M.-L. Tsai, *J. Neurosci. Methods* **2011**, *201*, 368.
- [86] P. Potejanasak, *Fifth Int. Conf. on Industrial Engineering and Applications (ICIEA)*, IEEE, Piscataway, NJ **2018**, pp. 199–202.
- [87] M. HajjHassan, V. Chodavarapu, S. Musallam, *Sensors* **2008**, *8*, 6704.
- [88] H. Takahashi, J. Suzurikawa, M. Nakao, F. Mase, K. Kaga, *IEEE Trans. Biomed. Eng.* **2005**, *52*, 952.
- [89] U.S. National Library of Medicine, *Stentrodé With Thought Controlled Digital Switch: An Early Feasibility Study (EFS) of the Safety of the Stentrodé Device in Participants With Loss of Motor Function Due to Paralysis From Spinal Cord Injury, Motor Neuron Disease, Stroke, Muscular Dystrophy or Loss of Limbs—Clinical Trial NCT03834857*, **2019**.
- [90] N. L. Opie, S. E. John, G. S. Rind, S. M. Ronayne, Y. T. Wong, G. Gerboni, P. E. Yoo, T. J. H. Lovell, T. C. M. Scordas, S. L. Wilson, A. Dornom, T. Vale, T. J. O'Brien, D. B. Grayden, C. N. May, T. J. Oxley, *Nat. Biomed. Eng.* **2018**, *2*, 907.
- [91] S. E. John, N. L. Opie, Y. T. Wong, G. S. Rind, S. M. Ronayne, G. Gerboni, S. H. Bauquier, T. J. O'Brien, C. N. May, D. B. Grayden, T. J. Oxley, *Sci. Rep.* **2018**, *8*, 8427.
- [92] A. Aldaoud, J. Redoute, K. Ganesan, G. S. Rind, S. E. John, S. M. Ronayne, N. L. Opie, D. J. Garrett, S. Prawer, *IEEE J. Electromagn., RF Microwaves Med. Biol.* **2018**, *2*, 193.
- [93] S. M. Strakowski, M. P. Delbello, C. M. Adler, *Mol. Psychiatry* **2005**, *10*, 105.
- [94] E. Schwarz, N. T. Doan, G. Pergola, L. T. Westlye, T. Kaufmann, T. Wolfers, R. Brecheisen, T. Quarto, A. J. Ing, P. D. Carlo, T. P. Gurholt, R. L. Harms, Q. Noirhomme, T. Moberget, I. Agartz, O. A. Andreassen, M. Bellani, A. Bertolino, G. Blasi, P. Brambilla, J. K. Buitelaar, S. Cervenka, L. Flyckt, S. Frangou, B. Franke, J. Hall, D. J. Heslenfeld, P. Kirsch, A. M. McIntosh, M. M. Nöthen, A. Papassotiropoulos, D. J.-F. de Quervain, M. Rietschel, G. Schumann, H. Tost, S. H. Witt, M. Zink, A. Meyer-Lindenberg, IMAGEMEND Consortium, Karolinska Schizophrenia Project (KaSP) Consortium, *Transl. Psychiatry* **2019**, *9*, 12.
- [95] N. E. Clifton, E. Hannon, J. C. Harwood, A. Di Florio, K. L. Thomas, P. A. Holmans, J. T. R. Walters, M. C. O'Donovan, M. J. Owen, A. J. Pocklington, J. Hall, *Transl. Psychiatry* **2019**, *9*, 74.

- [96] J. Muir, J. Lopez, R. C. Bagot, *Neuropsychopharmacology* **2019**, *44*, 1013.
- [97] D. M. Howard, M. J. Adams, T.-K. Clarke, J. D. Hafferty, J. Gibson, M. Shirali, J. R. I. Coleman, S. P. Hagenaaers, J. Ward, E. M. Wigmore, C. Alloza, X. Shen, M. C. Barbu, E. Y. Xu, H. C. Whalley, R. E. Marioni, D. J. Porteous, G. Davies, I. J. Deary, G. Hemani, K. Berger, H. Teismann, R. Rawal, V. Arolt, B. T. Baune, U. Dannlowski, K. Domschke, C. Tian, D. A. Hinds, 23 and Me Research Team, Major Depressive Disorder Working Group of the Psychiatric Genomics Consortium, M. Trzaskowski, E. M. Byrne, S. Ripke, D. J. Smith, P. F. Sullivan, N. R. Wray, G. Breen, C. M. Lewis, A. M. McIntosh, *Nat. Neurosci.* **2019**, *22*, 343.
- [98] M.-H. Lee, B. Siddoway, G. E. Kaeser, I. Segota, R. Rivera, W. J. Romanow, C. S. Liu, C. Park, G. Kennedy, T. Long, J. Chun, *Nature* **2018**, *563*, 639.
- [99] Probe|Neuropixels, <https://www.neuropixels.org/probe> (accessed: October 2018).
- [100] R. A. Falconer, S. L. Rogers, M. Shenai, *Front. Neurol.* **2018**, *9*, 544.
- [101] T. Zhou, G. Hong, T.-M. Fu, X. Yang, T. G. Schuhmann, R. D. Viveros, C. M. Lieber, *Proc. Natl. Acad. Sci. USA* **2017**, *114*, 5894.
- [102] T.-I. Kim, J. G. McCall, Y. H. Jung, X. Huang, E. R. Siuda, Y. Li, J. Song, Y. M. Song, H. A. Pao, R.-H. Kim, C. Lu, S. D. Lee, I.-S. Song, G. Shin, R. Al-Hasani, S. Kim, M. P. Tan, Y. Huang, F. G. Omenetto, J. A. Rogers, M. R. Bruchas, *Science* **2013**, *340*, 211.
- [103] P. Hickey, M. Stacy, *Front. Neurosci.* **2016**, *10*, 173.
- [104] M. Hariz, P. Blomstedt, L. Zrinzo, *Mov. Disord.* **2013**, *28*, 1784.
- [105] J. P. Seymour, F. Wu, K. D. Wise, E. Yoon, *Microsyst. Nanoeng.* **2017**, *3*, 16066.
- [106] R. J. Vetter, J. C. Williams, J. F. Hetke, E. A. Nunamaker, D. R. Kipke, *IEEE Trans. Biomed. Eng.* **2004**, *51*, 896.
- [107] R. J. Vetter, R. M. Miriani, B. E. Casey, K. Kong, J. F. Hetke, D. R. Kipke, *Conf. Proc. IEEE Eng. Med. Biol. Soc.* **2005**, *7*, 7341.
- [108] T. Moon, D. S. Pellinen, E. K. Purcell, J. P. Seymour, D. R. Kipke, in *World Congress on Medical Physics and Biomedical Engineering 2006* (Eds: R. Magjarevic, J. H. Nagel), Springer, Berlin **2007**, pp. 3542–3545.
- [109] R. Green, M. R. Abidian, *Adv. Mater.* **2015**, *27*, 7620.
- [110] B. Tian, J. Liu, T. Dvir, L. Jin, J. H. Tsui, Q. Qing, Z. Suo, R. Langer, D. S. Kohane, C. M. Lieber, *Nat. Mater.* **2012**, *11*, 986.
- [111] G. Hong, R. D. Viveros, T. J. Zwang, X. Yang, C. M. Lieber, *Biochemistry* **2018**, *57*, 3995.
- [112] F. Zhang, L.-P. Wang, E. S. Boyden, K. Deisseroth, *Nat. Methods* **2006**, *3*, 785.
- [113] S. H. Sunwoo, T.-I. Kim, in *Stretchable Bioelectronics for Medical Devices and Systems* (Eds: J. A. Rogers, R. Ghaffari, D.-H. Kim), Springer International Publishing, Cham **2016**, pp. 293–308.
- [114] B. Rubehn, S. B. E. Wolff, P. Tovote, A. Lüthi, T. Stieglitz, *Lab Chip* **2013**, *13*, 579.
- [115] Y. Son, H. J. Lee, J. Kim, H. Shin, N. Choi, C. J. Lee, E.-S. Yoon, E. Yoon, K. D. Wise, T. G. Kim, I.-J. Cho, *Sci. Rep.* **2015**, *5*, 15466.
- [116] K. L. Montgomery, A. J. Yeh, J. S. Ho, V. Tsao, S. Mohan Iyer, L. Grosenick, E. A. Ferenczi, Y. Tanabe, K. Deisseroth, S. L. Delp, A. S. Y. Poon, *Nat. Methods* **2015**, *12*, 969.
- [117] R. M. Neely, D. K. Piech, S. R. Santacruz, M. M. Maharbiz, J. M. Carmena, *Curr. Opin. Neurobiol.* **2018**, *50*, 64.
- [118] M. M. Maharbiz, *FDA Public Workshop—Orthopaedic Sensing, Measuring and Advanced Reporting Technology (SMART) Devices*, United States Food And Drug Administration, Silver Spring, MD **2018**.
- [119] G. Pinton, J.-F. Aubry, E. Bossy, M. Muller, M. Pernot, M. Tanter, *Med. Phys.* **2011**, *39*, 299.
- [120] C. A. Diaz-Botia, L. E. Luna, R. M. Neely, M. Chamanzar, C. Carraro, J. M. Carmena, P. N. Sabes, R. Maboudian, M. M. Maharbiz, *J. Neural Eng.* **2017**, *14*, 056006.
- [121] P. Köhler, A. Wolff, F. Ejserholm, L. Wallman, J. Schouenborg, C. E. Linsmeier, *PLoS One* **2015**, *10*, e0119340.
- [122] E. S. Erefej, G. M. Rial, J. K. Hermann, C. S. Smith, S. M. Meade, J. M. Rayyan, K. Chen, H. Feng, J. R. Capadona, *Front. Bioeng. Biotechnol.* **2018**, *6*, 9.
- [123] R. R. Shamir, A. Zaidel, L. Joskowicz, H. Bergman, Z. Israel, *Stereotact. Funct. Neurosurg.* **2012**, *90*, 325.
- [124] Z. Li, J.-G. Zhang, Y. Ye, X. Li, *Stereotact. Funct. Neurosurg.* **2016**, *94*, 351.
- [125] I. S. Kourbeti, A. F. Vakis, P. Ziakas, D. Karabetos, E. Potosidis, S. Christou, G. Samonis, *J. Neurosurg.* **2015**, *122*, 1113.
- [126] T. D. Y. Kozai, D. R. Kipke, *J. Neurosci. Methods* **2009**, *184*, 199.
- [127] A. Hess-Dunning, D. J. Tyler, *Micromachines* **2018**, *9*, 583.
- [128] T. Suzuki, K. Mabuchi, S. Takeuchi, *First Int. IEEE EMBS Conf. on Neural Engineering, 2003*, IEEE, Piscataway, NJ, **2003**, pp. 154–156.
- [129] F. Wu, M. Im, E. Yoon, *16th Int. Solid-State Sensors, Actuators and Microsystems Conf.*, Transducers, Beijing **2011**, pp. 966–969.
- [130] P. J. Gilgunn, R. Khilwani, T. D. Y. Kozai, D. J. Weber, X. T. Cui, G. Erdos, O. B. Ozdoganlar, G. K. Fedder, *25th IEEE Int. Conf. on Micro Electro Mechanical Systems (MEMS)*, IEEE, Piscataway, NJ **2012**, pp. 56–59.
- [131] M. Jeon, J. Cho, Y. K. Kim, D. Jung, E.-S. Yoon, S. Shin, I.-J. Cho, *J. Micromech. Microeng.* **2014**, *24*, 025010.
- [132] X. Wen, B. Wang, S. Huang, T. “leo” Liu, M.-S. Lee, P.-S. Chung, Y. T. Chow, I.-W. Huang, H. G. Monbouquette, N. T. Maidment, P.-Y. Chiou, *Biosens. Bioelectron.* **2019**, *131*, 37.
- [133] T. D. Y. Kozai, Z. Gugel, X. Li, P. J. Gilgunn, R. Khilwani, O. B. Ozdoganlar, G. K. Fedder, D. J. Weber, X. T. Cui, *Biomaterials* **2014**, *35*, 9255.
- [134] F. Barz, P. Ruther, S. Takeuchi, O. Paul, *28th IEEE Int. Conf. on Micro Electro Mechanical Systems (MEMS)*, IEEE, Piscataway, NJ **2015**, pp. 636–639.
- [135] R. Khilwani, P. J. Gilgunn, T. D. Y. Kozai, X. C. Ong, E. Korkmaz, P. K. Gunalan, X. T. Cui, G. K. Fedder, O. B. Ozdoganlar, *Biomed. Microdevices* **2016**, *18*, 97.
- [136] T. G. Schuhmann Jr., T. Zhou, G. Hong, J. M. Lee, T.-M. Fu, H.-G. Park, C. M. Lieber, *J. Visualized Exp.* **2018**, *137*, E58003.
- [137] E. Strickland, *IEEE Spectrum*, <https://spectrum.ieee.org/the-human-os/biomedical/devices/5-neuroscience-experts-weigh-in-on-elon-musk-s-mysterious-neural-lace-company> (accessed: March 2019).
- [138] M. Ghazanwy, R. Chakrabarti, A. Tewari, A. Sinha, *Saudi J. Anaesth.* **2014**, *8*, 529.
- [139] J. C. Barrese, N. Rao, K. Paroo, C. Triebwasser, C. Vargas-Irwin, L. Franquemont, J. P. Donoghue, *J. Neural Eng.* **2013**, *10*, 066014.
- [140] V. S. Polikov, P. A. Tresco, W. M. Reichert, *J. Neurosci. Methods* **2005**, *148*, 1.
- [141] T. D. Y. Kozai, A. S. Jaquins-Gerstl, A. L. Vazquez, A. C. Michael, X. T. Cui, *ACS Chem. Neurosci.* **2015**, *6*, 48.
- [142] H. Hämmerle, K. Kobuch, K. Kohler, W. Nisch, H. Sachs, M. Stelzle, *Biomaterials* **2002**, *23*, 797.
- [143] E. Patrick, M. E. Orazem, J. C. Sanchez, T. Nishida, *J. Neurosci. Methods* **2011**, *198*, 158.
- [144] T. Saxena, L. Karumbaiah, E. A. Gaupp, R. Patkar, K. Patil, M. Betancur, G. B. Stanley, R. V. Bellamkonda, *Biomaterials* **2013**, *34*, 4703.
- [145] D. H. Szarowski, M. D. Andersen, S. Retterer, A. J. Spence, M. Isaacson, H. G. Craighead, J. N. Turner, W. Shain, *Brain Res.* **2003**, *983*, 23.
- [146] A. D. Degenhart, J. Eles, R. Dum, J. L. Mischel, I. Smalianchuk, B. Endler, R. C. Ashmore, E. C. Tyler-Kabara, N. G. Hatsopoulos, W. Wang, A. P. Batista, X. T. Cui, *J. Neural Eng.* **2016**, *13*, 046019.
- [147] S. L. Chamberlin, T. Gale, B. Narins, *Choice Rev. Online* **2005**, *10*, 42.

- [148] P. Blomstedt, H. Bjartmarz, *Stereotact. Funct. Neurosurg.* **2012**, *90*, 92.
- [149] J. A. Coles, P. J. Stewart-Hutchinson, E. Myburgh, J. M. Brewer, *Methods* **2017**, *127*, 53.
- [150] J. C. Barrese, J. Aceros, J. P. Donoghue, *J. Neural Eng.* **2016**, *13*, 026003.
- [151] S. Bjerknes, I. M. Skogseid, T. Sæhle, E. Dietrichs, M. Toft, *PLoS One* **2014**, *9*, e105288.
- [152] T. Escamilla-Mackert, N. B. Langhals, T. D. Y. Kozai, D. R. Kipke, *Conf. Proc. IEEE Eng. Med. Biol. Soc.* **2009**, *2009*, 1616.
- [153] T. Morishita, J. D. Hilliard, M. S. Okun, D. Neal, K. A. Nestor, D. Peace, A. A. Hozouri, M. R. Davidson, F. J. Bova, J. M. Sporrer, G. Oyama, K. D. Foote, *PLoS One* **2017**, *12*, e0183711.
- [154] J. Y. Sim, M. P. Haney, S. I. Park, J. G. McCall, J.-W. Jeong, *Lab Chip* **2017**, *17*, 1406.
- [155] A. Lecomte, E. Descamps, C. Bergaud, *J. Neural Eng.* **2018**, *15*, 031001.
- [156] G. C. McConnell, H. D. Rees, A. I. Levey, C.-A. Gutekunst, R. E. Gross, R. V. Bellamkonda, *J. Neural Eng.* **2009**, *6*, 056003.
- [157] R. Biran, D. C. Martin, P. A. Tresco, *Exp. Neurol.* **2005**, *195*, 115.
- [158] A. B. Schwartz, X. T. Cui, D. J. Weber, D. W. Moran, *Neuron* **2006**, *52*, 205.
- [159] M. A. M. Freire, E. Morya, J. Faber, J. R. Santos, J. S. Guimaraes, N. A. M. Lemos, K. Sameshima, A. Pereira, S. Ribeiro, M. A. L. Nicolelis, *PLoS One* **2011**, *6*, e27554.
- [160] J. L. Collinger, B. Wodlinger, J. E. Downey, W. Wang, E. C. Tyler-Kabara, D. J. Weber, A. J. C. McMorland, M. Velliste, M. L. Boninger, A. B. Schwartz, *Lancet* **2013**, *381*, 557.
- [161] A. Wang, P. G. Finlayson, J. Li, K. Brabant, C. A. Black, J. P. McAllister II, T. Cao, H. Tang, X. Liang, S. O. Salley, G. W. Auner, K. Y. S. Ng, presented at *American Institute of Chemical Engineering Annu. Meet.*, Cincinnati, OH, October **2005**.
- [162] A. V. Kaplan, D. S. Baim, J. J. Smith, D. A. Feigal, M. Simons, D. Jefferys, T. J. Fogarty, R. E. Kuntz, M. B. Leon, *Circulation* **2004**, *109*, 3068.
- [163] D.-B. Tillman, *Letter to Patrick L. Johnson, Medtronic Neuromodulation*, United States Food And Drug Administration, Silver Spring, MD **2009**.
- [164] V. Gilja, C. Pandarinath, C. H. Blabe, P. Nuyujukian, J. D. Simeral, A. A. Sarma, B. L. Soric, J. A. Perge, B. Jarosiewicz, L. R. Hochberg, K. V. Shenoy, J. M. Henderson, *Nat. Med.* **2015**, *21*, 1142.
- [165] J. L. Contreras-Vidal, in *FDA Public Workshop—Brain—Computer Interface (BCI) Devices for Patients with Paralysis and Amputation*, United States Food And Drug Administration, Silver Spring, MD **2014**.
- [166] J. Zhang, T. Wang, C.-C. Zhang, K. Zeljic, S. Zhan, B.-M. Sun, D.-Y. Li, *Clin. Interventions Aging* **2017**, *12*, 923.
- [167] A. J. Fenoy, R. K. Simpson Jr., *J. Neurosurg.* **2014**, *120*, 132.
- [168] R. Voelker, *JAMA, J. Am. Med. Assoc.* **2015**, *314*, 443.
- [169] United States Food and Drug Administration, *Class 2 Device Recall, Blackrock Microsystems, Inserter Wand Holder for NeuroPort Array Brain Monitoring Device*, ID 55304, **2010**.
- [170] United States Food and Drug Administration, *Class 1 Device Recall, Ad-Tech Medical Macro Micro Subdural Electrodes*, ID 64136, **2013**.
- [171] United States Food and Drug Administration, *Class 2 Device Recall, Ad-Tech Medical Cueva Electrode Kit*, ID 69436, **2014**.
- [172] United States Food and Drug Administration, *Class 2 Device Recall, FHC microTargeting Guideline 4000 Ver 1.4 (GL4K) Software*, ID 54278, **2010**.
- [173] United States Food and Drug Administration, *Class 1 Device Recall, Medtronic, Inc., Activa Dystonia Therapy Kit*, ID 64439, **2013**.
- [174] United States Food and Drug Administration, *Class 2 Device Recall, Integra Life Sciences Ojemann Cortical Stimulator*, ID 64665, **2013**.
- [175] D. M. Zuckerman, P. Brown, S. E. Nissen, *Arch. Intern. Med.* **2011**, *171*, 1006.
- [176] D. W. L. Hukins, A. Mahomed, S. N. Kukureka, *Med. Eng. Phys.* **2008**, *30*, 1270.
- [177] D. J. DiLorenzo, J. Jankovic, R. K. Simpson, H. Takei, S. Z. Powell, *Neuromodulation* **2014**, *17*, 405.
- [178] A. Rothman, S. Davidson, R. G. Wiencek, W. N. Evans, H. Restrepo, V. Sarukhanov, E. Ruoslahti, R. Williams, D. Mann, *Pulm. Circ.* **2013**, *3*, 50.
- [179] B. W. Kristensen, J. Noraberg, P. Thiébaud, M. Koudelka-Hep, J. Zimmer, *Brain Res.* **2001**, *896*, 1.
- [180] L. A. Geddes, R. Roeder, *Ann. Biomed. Eng.* **2003**, *31*, 879.
- [181] M. Han, D. B. McCreery, *Conf. Proc. IEEE Eng. Med. Biol. Soc.* **2008**, *2008*, 4220.
- [182] S. Kuppusami, R. H. Oskouei, *Univers. J. Biomed. Eng.* **2015**, *3*, 9.
- [183] M. Asplund, E. Thaning, J. Lundberg, A. C. Sandberg-Nordqvist, B. Kostyszyn, O. Inganäs, H. von Holst, *Biomed. Mater.* **2009**, *4*, 045009.
- [184] United States Food and Drug Administration, *GYA Product Classification, EEG Lead, Class I*, **2019**.
- [185] United States Food and Drug Administration, *510(k) Summary, World Precision Instruments Dermtrode, ID K883869*, **1988**.
- [186] United States Food and Drug Administration, *HCD Product Classification, Ventricular Cannula, Class I*, **2019**.
- [187] United States Food and Drug Administration, *United States Food and Drug Administration, GYC Product Classification, Cortical Electrode, Class II*, **2019**.
- [188] United States Food and Drug Administration, *510(k) Summary, Micromed Cortical Electrode, ID K180761*, **2018**.
- [189] United States Food and Drug Administration, *IKD Product Classification, Cable, Electrode, Class II*, **2019**.
- [190] United States Food and Drug Administration, *GZL Product Classification, Depth Electrode, Class II*, **2019**.
- [191] United States Food and Drug Administration, *510(k) Summary, Dixi Medical Depth Electrode, ID K170959*, **2017**.
- [192] United States Food and Drug Administration, *OMA Product Classification, Amplitude-Integrated Electroencephalograph, Class II*, **2019**.
- [193] United States Food and Drug Administration, *510(k) Summary, Nihon Kohden Corporation Amplitude-Integrated Electroencephalograph, ID K130238*, **2015**.
- [194] United States Food and Drug Administration, *PFN Product Classification, Implanted Brain Stimulator for Epilepsy, Class III*, **2019**.
- [195] United States Food and Drug Administration, *PIM Product Classification, Neuromodulator for Obesity, Class III*, **2019**.
- [196] United States Food and Drug Administration, *Pre-Market Approval (PMA) Summary, ReShape Lifesciences, Inc., Neuromodulator for Obesity, ID P130019*, **2015**.
- [197] United States Food and Drug Administration, *NHL Product Classification, Implanted Electrical Stimulator for Parkinsonian Systems, Class III*, **2019**.
- [198] United States Food and Drug Administration, *Pre-Market Approval (PMA) Summary, Abbott Medical Implanted Electrical Stimulator for Parkinsonian Tremor, ID P140009/S044*, **2019**.
- [199] T. R. Clites, H. M. Herr, S. S. Srinivasan, A. N. Zorzos, M. J. Carty, *Plast. Reconstr. Surg.—Global Open* **2018**, *6*, e1997.
- [200] Center for Devices and Radiological Health, *About the Center for Devices and Radiological Health—External Expertise and Partnerships (EEP)*, **2018**.
- [201] United States Food and Drug Administration, *Agenda for Quarterly Meeting on MDUFA IV (FY 2018–2022) Performance*, **2018**.
- [202] E. Chan, *John M. Marshall J. Inf. Technol. Privacy Law* **2007**, *25*, 4.
- [203] Vascular News, *Europe Braces for Harder Times in Medical Device Innovation while US FDA Eases Regulations*, **2018**.
- [204] G. A. Van Norman, *JACC* **2016**, *1*, 399.
- [205] ECA Academy, *What are the Differences between EU and FDA GMP?*, **2018**.
- [206] Emergo, *Japan Regulatory Approval Process for Medical Devices*, **2013**.
- [207] M. W. Krucoff, *Harmonization by Doing (HBD) East 2017 Think Tank Meet.*, Japan Pharmaceuticals And Medical Devices Agency, Tokyo, Japan **2017**.